frontiers | Frontiers in Earth Science

TYPE Original Research
PUBLISHED 11 January 2024
DOI 10.3389/feart.2023.1231984

OPEN ACCESS

EDITED BY
Lawrence H. Tanner,
Le Moyne College, United States

REVIEWED BY
Vahid Tavakoli,
University of Tehran, Iran
Kei Ogata,
University of Naples Federico II, Italy

*CORRESPONDENCE
Haiteng Zhuo,
zhuoht3@mail.sysu.edu.cn

RECEIVED 31 May 2023
ACCEPTED 15 December 2023
PUBLISHED 11 January 2024

CITATION
Chen W, Liu J, Peng G, Wei Z, Jia P, Yao J, Wang Z and Zhuo H (2024), Stratigraphic-sedimentary evolution of a mixed siliciclastic-carbonate system in the Huizhou Sag of the Pearl River Mouth Basin, Northern South China Sea.
Front. Earth Sci. 11:1231984.
doi: 10.3389/feart.2023.1231984

Stratigraphic-sedimentary evolution of a mixed siliciclastic-carbonate system in the Huizhou Sag of the Pearl River Mouth Basin, Northern South China Sea

Weitao Chen[1], Jun Liu[1], Guangrong Peng[1], Zhe Wei[1], Peimeng Jia[1], Jiali Yao[1], Zhina Wang[2] and Haiteng Zhuo[2,3,4]*

[1]Shenzhen Branch of CNOOC Limited, Shenzhen, China, [2]School of Marine Sciences, Sun Yat-sen University, Zhuhai, China, [3]Southern Marine Science and Engineering Guangdong Laboratory (Zhuhai), Zhuhai, China, [4]Guangdong Provincial Key Laboratory of Marine Resources and Coastal Engineering, Sun Yat-sen University, Guangzhou, China

Mixed siliciclastic-carbonate systems are regulated interactively by factors such as siliciclastic sediment supply, carbonate production, sea-level change, tectonism, and climate conditions. These systems record vital information that aids in understanding ancient environments. This study used a merged 3D seismic volume, in conjunction with over 100 industrial wells, to systematically investigate the stratigraphic-sedimentary evolution of such a system within the Huizhou Sag of the Pearl River Mouth Basin, located on the northern continental shelf of the South China Sea. In total, six major sequence boundaries were identified for the Zhujiang Formation within the area, thus subdividing the interval into five typical third-order depositional sequences. Each of these sequences can be divided into a transgressive and a highstand systems tract. Lowstand or falling stage systems tracts were also recognized, the deposition of which was potentially in response to the uplifting process of the Dongsha Rise. During the deposition of the Zhujiang Formation, the Huizhou Sag may have undergone a sequential evolutionary history from delta-shore, to delta-shore-tidal-lagoon, to delta-shore-carbonate, and finally to delta-shore-shallow marine systems. This evolution responded to a varying degree of mixing processes, which was mainly regulated by siliciclastic sediment supply, confined paleomorphology, and local oceanic currents. Furthermore, the deposition of the Zhujiang Formation in the Huizhou Area was time-equivalent with the spreading process after the ridge jump of the South China Sea (23–16.5 Ma), providing valuable insights into sea-level fluctuations, provenance changes, and tectonic evolution. Our results may also shed light on the evaluation of lithologic traps and hydrocarbon sweet spots within mixed siliciclastic-carbonate systems.

KEYWORDS

mixed siliciclastic-carbonate system, sequence stratigraphy, South China Sea, Pearl River Mouth Basin, stratigraphic traps

1 Introduction

The stratigraphy and sedimentation of mixed siliciclastic-carbonate systems are characterized by the co-occurrence of two fundamentally different developing mechanisms, which are mainly controlled by siliciclastic and carbonate sediment supply (Mount, 1984). Besides, other intra- and extra-basinal factors such as sea-level change, regional or local tectonics, and climatic change, can further complicate these mixed systems (Zonneveld et al., 2012; Zecchin and Catuneanu, 2017). For example, due to the existence of local fluvial input, the interaction of siliciclastic-carbonate systems can vary significantly in both spatial or temporal perspectives (Mount, 1984; Zonneveld et al., 2012).

A mixed system of siliciclastic-carbonate has been identified on the northern shelf of the South China Sea, spanning from the Huizhou Sag to the Dongsha Rise, as reported by Zhang et al. (2021). During the deposition of the Zhujiang Formation, the ancient Pearl River Delta started to interact with the ancient carbonate platform system, a process that occurred approximately between 23–16.5 Ma (Chen et al., 2012; Chen et al., 2016; Wei et al., 2022). This system has been statistically proven to contain the most abundant oil fields in the eastern part of the Pearl River Mouth Basin of the South China Sea (Shi et al., 2008; Shi et al., 2009; Shi et al., 2015). The Zhujiang Formation, which is the primary producing reservoir and exhibits the highest degree of mixing processes, holds roughly over 90% of the total oil and gas reserves (Chen et al., 2003).

In recent years, owing to the escalating challenges in discovering structural traps, the exploration potential of stratigraphic-lithologic traps has progressively captured the attention of researchers (Long et al., 2006; Dong et al., 2008; Chen et al., 2012; Chen et al., 2016; Du et al., 2014; Shabani et al., 2022; Shabani et al., 2023). Interestingly, it has been observed that the largest stratigraphic traps are often associated, to some degree, with this mixed siliciclastic-carbonate system (Zhang et al., 2021). Consequently, a detailed stratigraphic and sedimentary study was conducted in this study to gain a better understanding of this mixed system. The study also aimed to elucidate how regional or local factors, such as paleo-sea-level, paleo-climate, and paleo-tectonism, dictate the evolution of this mixed system on the northern margin of the South China Sea.

The earliest sequence stratigraphic scheme for the Pearl River Delta and the Huizhou Area was established as far back as 1989, and it was complemented by a high-resolution sea-level curve derived from coastal analysis (Qin, 1996; Qin, 2002; Chen et al., 2003; Dong et al., 2008; Liu et al., 2011; He et al., 2017). Following the final breakup of the continental crust around 30 Ma, the entire northern margin transitioned into a passive-margin stage (Pang et al., 2007a; Pang et al., 2007b; Shao et al., 2008; Zhuo et al., 2019). Since then, the Zhu I Depression, where the Huizhou Area is situated, has been dominated by delta and coastal systems. Based on seismic stratigraphy and samples obtained from select key boreholes, the sea-level curve constructed by Qin (1996) displayed a divergence from the global curve published by Haq et al. (1987). Since 33 Ma, the Pearl River Mouth Basin has shown a consistent pattern of transgression, which may stand in contrast to patterns observed in other basins (Qin, 1996).

Numerous studies have highlighted that the northern shelf region of the South China Sea is influenced by intricate hydrodynamic conditions, encompassing coastal currents, monsoon drift, and the shelf intrusion current of the South China Sea Branch of Kuroshio (Liu et al., 2011; Zhuo et al., 2014; He et al., 2017). These complex hydrodynamic processes have a significant impact on the delta-shelf system as well as the mixed sedimentation (He et al., 2017). Currently, there is a wealth of research examining the control effect of hydrodynamics on sedimentation since the Hanjiang period (ca. 16.5 Ma), in contrast, studies focusing on the Zhujiang Formation (ca. 23–16.5 Ma) are relatively scarce (Zhuo et al., 2014; He et al., 2017). In this study, we utilize an integrated subsurface dataset comprised of 3D seismic volumes, well data, and cores. Our objectives are threefold: 1) delineate the sequence stratigraphy and reconstruct the depositional evolution of the Zhujiang Formation; 2) investigate the interplay between terrigenous clastic influx and carbonate system dynamics; and 3) unravel the determinants that govern the evolution and final disposition of these depositional systems.

2 Geological background

The South China Sea is located at the junction of the Eurasian, Pacific, and Indian plates and is one of the largest marginal seas along the western margin of the Pacific Ocean (Zhong, 1994; Zhang et al., 2007; Sun et al., 2009). The Huizhou Area, situated at the center of the Pearl River Mouth Basin in the northern shelf region of the South China Sea's northern margin, encompasses the southeast portion of the Huizhou Sag and the northwest portion of the Dongsha Rise (Figures 1, 2). The sedimentary environment of the Huizhou Area is intimately linked to the tectonic evolution of the South China Sea basin (Gong et al., 1997).

During the rifting stage (ca. 66–33.9 Ma), numerous rift lake basins with strong segmentation were developed, creating favorable conditions for source rock deposition in the basin (Gong et al., 1997). Along with the Nanhai Movement at ca. 33.9 Ma (Figure 3), the northern part of the South China Sea began to enter the post-rift stage. Since then, seawater gradually invaded the northern continental margin of the South China Sea and a lot of marginal to deep marine facies began to form within the study area. At this stage, seawater intruded into the Zhu II Depression (Figure 2), with the shelf area primarily characterized by braided river deltas and shallow marine depositional systems (He et al., 2017).

The Baiyun Movement occurred at ca. 23 Ma (Figure 3), directly leading to the northward migration of the shelf edge (Pang et al., 2005; Pang et al., 2007a; Pang et al., 2007b; Zhuo et al., 2019). Seawater invaded the Zhu I Depression. A significant amount of terrigenous clastic materials was transported and delivered to the Huizhou Sag from the west forming the Pearl River Delta in Zhujiang Formation between 23.8 and 16.5 Ma (Figure 2). After ca. 21 Ma, the carbonate platform began to grow rapidly atop the Dongsha Rise (Figures 1, 3), until about 17.5 Ma, when the platform was submerged owing to marine transgression. Notably, in certain local high areas, the development of carbonate platforms continues even to this day. The Dongsha Rise was exposed and eroded during the Paleogene period. Its periphery and the Dongsha Rise area saw the development of various types of sedimentary systems, such as shore, tidal-lagoon, and carbonate platform, at different stages and to varying degrees (Chen et al., 2012).

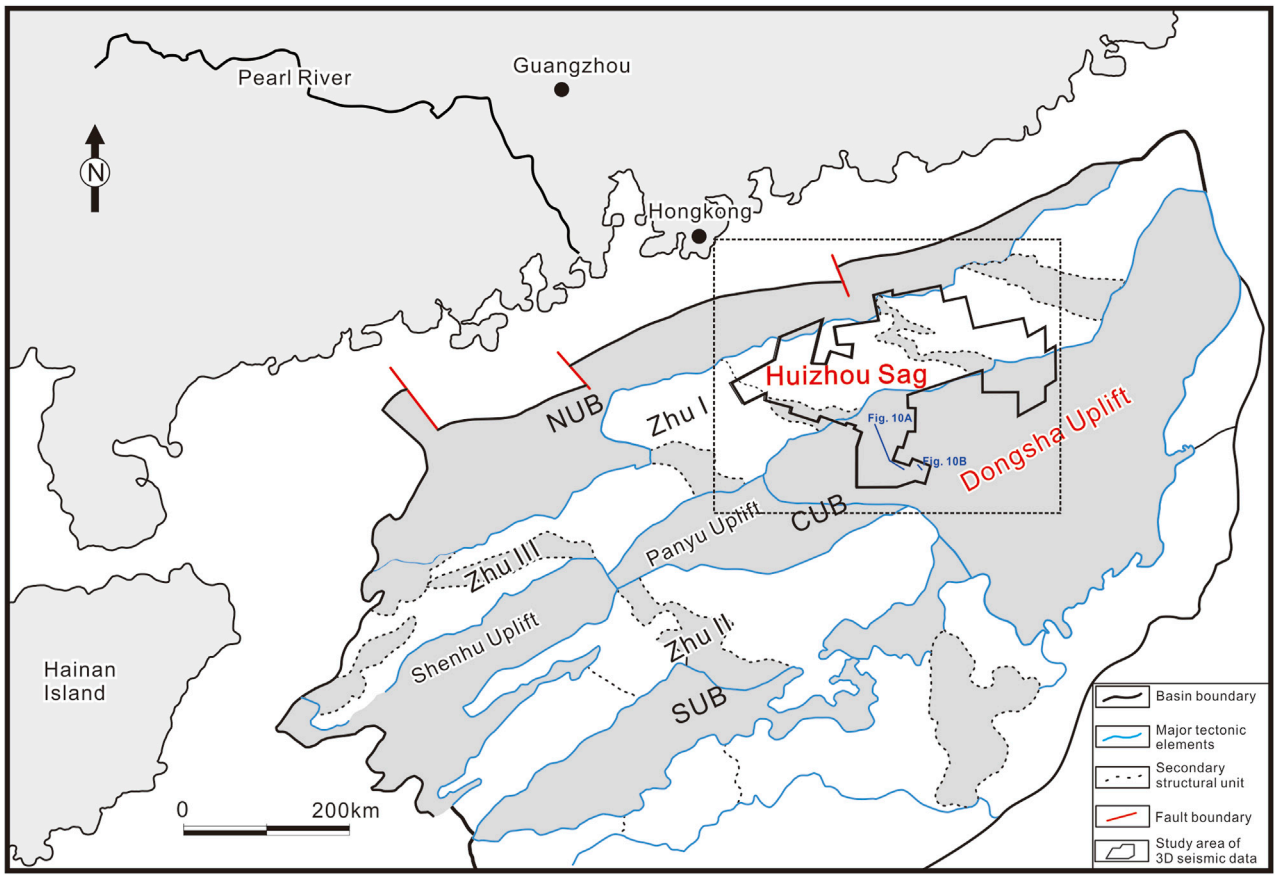

FIGURE 1
Location map showing major tectonic elements of the Pearl River Mouth Bain. Note the locations of the Zhu I Depression and the Huizhou Sag. Also note the 3D seismic survey used in this study. Abbreviations: Zhu I, Zhu I Depression; Zhu I, Zhu II Depression; Zhu III, Zhu III Depression; NUB, Northern Uplifting Belt; CUB, Central Uplifting Belt; SUB, Southern Uplifting Belt.

At ca. 16 Ma, the South China Sea stopped its seafloor spreading marked by the closure of Indonesian Seaway (Figure 3) and marine transgression was intensified hereafter (Gong et al., 1997). The subsequent deposition of the Hanjiang Formation was mainly dominated by deltaic and shallow marine facies, but the size of the delta was significantly smaller, especially after ca. 13.8 Ma (He et al., 2017). Previous studies have shown that the 13.8 Ma interface is marked by a dramatic reglaciation of the Antarctic ice sheet, sea-level drop, neo-tectonism, and monsoon evolution (He et al., 2017).

Around 10.5 Ma, the Dongsha Movement (Figure 3) took place in the northern part of the South China Sea and persisted until 5.5 Ma. This event profoundly influenced the tectonic and sedimentary patterns in and around the study area. During this time, the deposition of the Yuehai and Wanshan Formations was predominantly characterized by shallow marine facies. This led to an additional retreat of the entire Pearl River Delta depositional system (Pang et al., 2007b).

3 Data and methods

This study is based on the interpretation of an integrated dataset comprising well logs from 127 industrial wells, tens of meters of cores with paleontological data, and a merged 3D seismic volume. Firstly, major sequence boundaries across the study area were recognized and traced (Figures 4, 5), according to basic workflows of seismic stratigraphy (Mitchum et al., 1977; Vail et al., 1977; Van Wagoner et al., 1988) and sequence stratigraphy (Posamentier and Allen, 1999; Catuneanu, 2006; Catuneanu et al., 2009; Neal and Abreu, 2009). Seismic facies types and their recognition criteria were summarized using a combination of core descriptions, well log patterns, and seismic facies analysis. Furthermore, aided by the extraction of RMS amplitudes, the distribution of the sedimentary facies was mapped herein to reconstruct the depositional history of the entire study area. Subsequently, we discussed and identified the primary forcing factors that govern the stratigraphic-sedimentary evolution of the study area.

4 Results

4.1 Sequence stratigraphy

4.1.1 Sequence boundaries (SBs)

On seismic profiles, there are some truncated and incised features in the local area, indicating the presence of SBs (Figure 4). These incisions are overall disconnected and formed

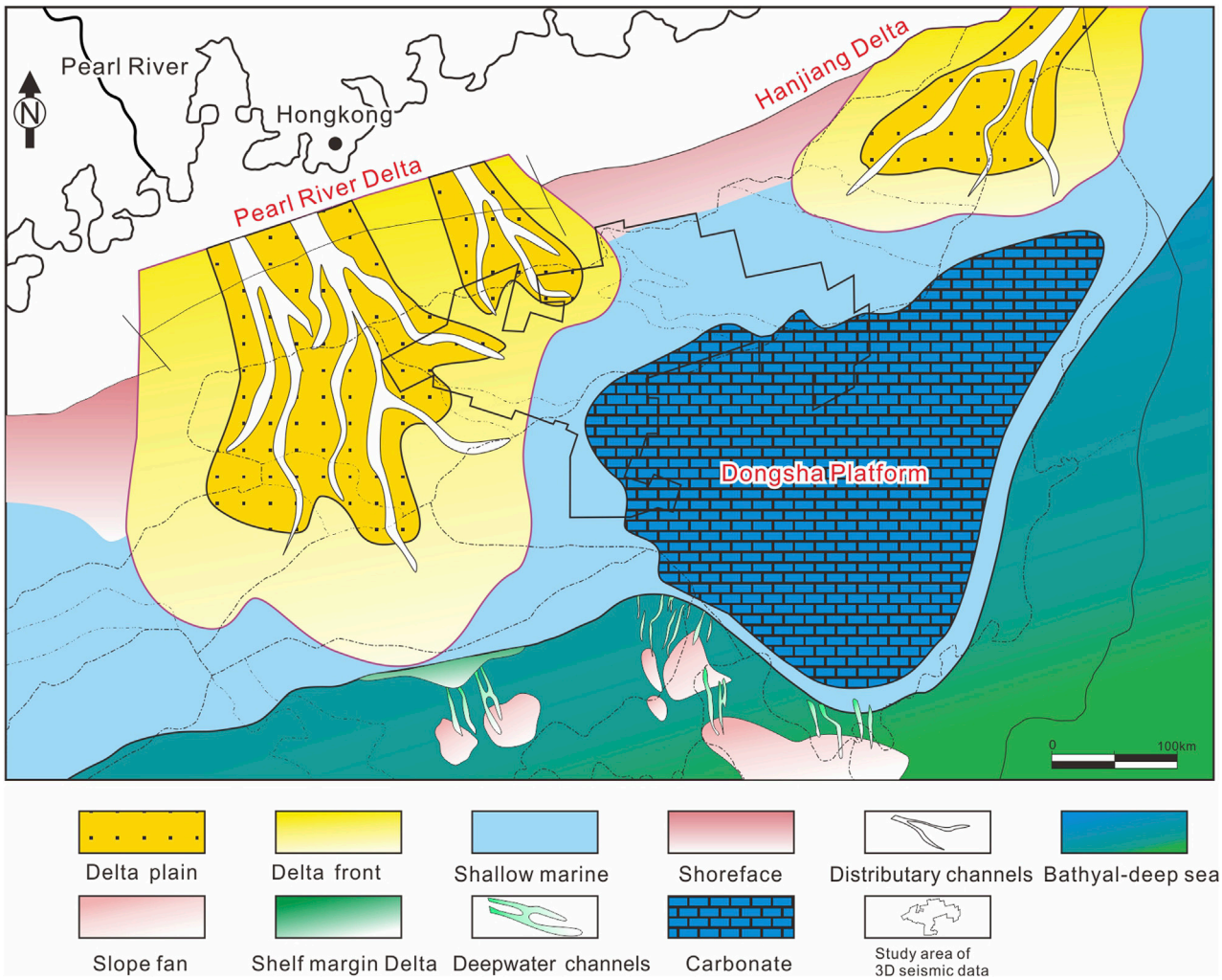

FIGURE 2
Paleogeographic reconstructions showing the distribution of depositional environments around the Dongsha Platform during the deposition of the Zhujiang Formation. The study area was jointly influenced by three major depositional systems, including the Pearl River Delta, the Hanjiang Delta, and the Dongsha Platform.

an analogy U-shaped undercutting (Figure 4C). Most sequence boundaries have toplap reflection below the interface (Figure 4), and onlaps can be observed above the SBs. It should be noted that truncation only developed in the western part of the Dongsha Rise, the northern region of the Huizhou Depression, and the Huizhou Low Rise in the study area (Figure 2).

From well logs, SBs display three different patterns, largely due to the variability of sedimentary facies in different areas (Figures 5–7):

Scenario I: the SBs separate a coarsening-up sandy interval below from a fining-upward sandy interval above (Figures 5–7). Below the boundary is a reverse cycle in which the number of sandstones increases upward, the proportion of argillaceous rocks decreases, and the amplitude of electrical curves increases upward. Above the boundary is a positive cycle in which the amount of sandstone decreases upward, the proportion of argillaceous rocks increases, and the amplitude of electrical curves decreases upward. The characteristics of this sequence boundary reflect the highstand systems tract (HST) of the underlying sequence and the transgressive tract of the overlying sequence. Moreover, the erosion near the sequence boundary is either minimal or nonexistent.

Scenario II: the SBs separate a muddy interval below from a coarsening-up sandy interval above (Figures 5–7). Below the boundary is a succession of mudstone, with the amplitude of the electrical curve being small. Above the boundary is a fining-upward cycle where the amount of sandstone decreases upward, the proportion of argillaceous rocks increases, and the values of the electrical curve decrease upward, indicating the presence of Transgressive Systems Tract (TST) deposits. This suggests two possibilities: (i) the sand-rich section in the underlying Highstand Systems Tract (HST) had been eroded, leaving only the mudstone section formed in the early stage of the HST, or (ii) the underlying HST deposits formed due to the dominant supply of muddy sediments. There is a certain difference in the characteristics of the underlying mudstone in these two scenarios. The former has a large number of markers indicating shallow water and oxidation exposure, while the latter is mudstone formed in deep water.

Scenario III: the SBs separate a coarsening-up sandy interval below from a serrated muddy interval above (Figures 5–7). Below the

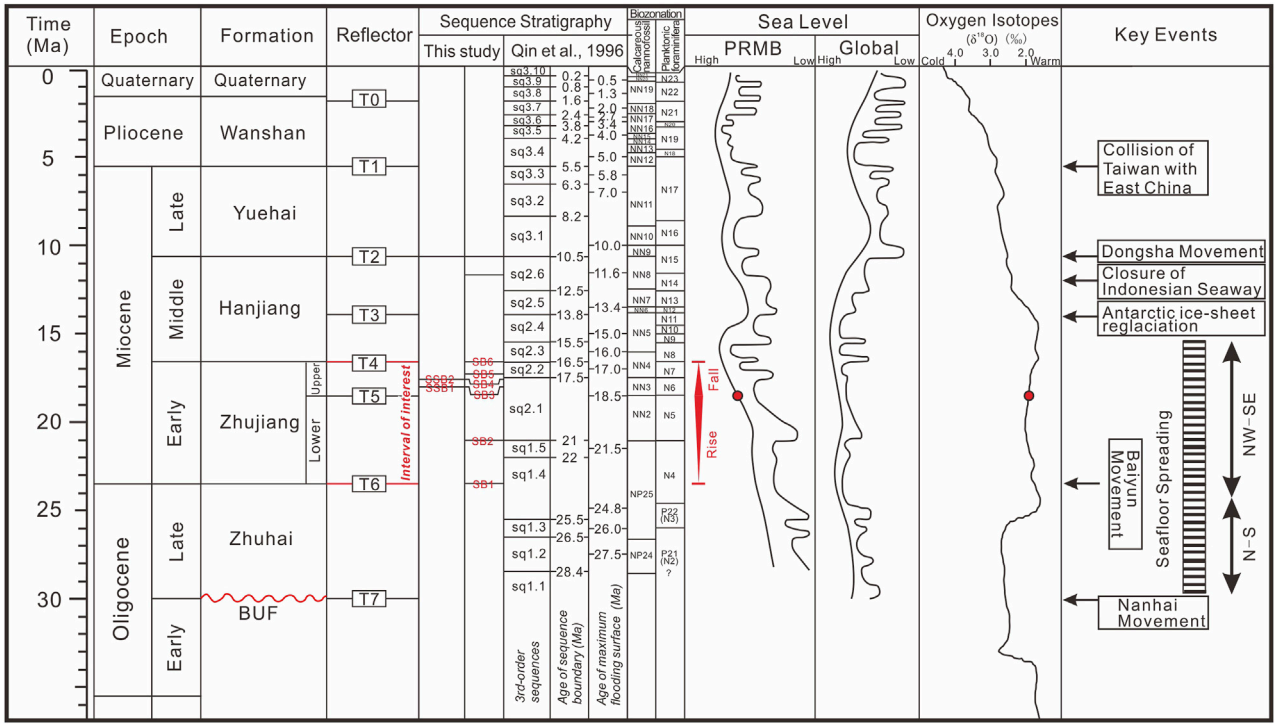

FIGURE 3
Comprehensive stratigraphic columns showing the sequence stratigraphic subdivisions of this study. The biozonation is from Qin. (1996). The local and global sea-level curves are from Qin. (1996) and Haq et al. (1987), respectively. Key tectonic and palaeoceanographic events are according to Gong et al. (1997), Zhuo et al. (2014), and He et al. (2017).

boundary, a reverse cycle exists where sandstones increase upward, argillaceous rocks decrease, and the amplitude of electrical curves increases upward. Above the boundary is a mudstone section, characterized by a predominantly serrated electrical curve with a small amplitude. This characteristic of the sequence boundary reflects an abundant supply of terrigenous sandy coarse debris in the HST of the underlying sequence, and a significant supply of terrigenous clasts, primarily argillaceous, in the transgressive system tract (TST) of the overlying sequence. During the HST period, the sufficient supply of terrigenous sandy coarse debris led to a gradual shallowing of the water body as the shoreline migrated seaward, forming a coarsening-upward cycle below the boundary, where the sandstone content gradually increased and the argillaceous content gradually decreased. Conversely, during the TST period, the terrigenous clastic supply was primarily argillaceous, and the water body deepened as the shoreline migrated landward, forming mudstone sections with progressively darker colors above the boundary.

From core data, third-order SBs displayed shoaling water, subaerial exposure, and erosion on core data. The diagnostic feature for water shoaling upward is the presence of calcareous mudstone (Figure 8). Erosion and channel incision occurred were characterized by scour surface (Tavakoli et al., 2018) (Figure 8).

4.1.2 Maximum flooding surfaces (MFSs)

On the seismic section, MFSs are mainly manifested as a low-frequency, highly continuous, and high-amplitude reflections (Figures 5–7). In some areas, the downlaping pattern of the overlying strata and the truncation of underlying strata can be observed (Figures 5–7). On well logs, the MFS was characterized by high gamma value, which separated a fining-upward cycle below and a coarsening-upward cycle above (Tavakoli, 2017). In lithology, MFS lies within a mudstone section, where the abundance of planktonic foraminifera is the maximum.

4.1.3 Stratigraphic organizations

According to the recognition of SBs and MFSs, the Zhujiang Formation in the study area can be subdivided into five third-order sequences (Figures 5–7). To establish a high-resolution stratigraphic framework, ten systems tracts are further delineated using the sequence boundaries and maximum flooding surfaces within the Zhujiang Formation, primarily dominated by the TSTs and HSTs. Notably, a lowstand systems tract is recognized in the Pearl River Delta system due to the influence of local slope breaks, which provide some local accommodation for the deposition and preservation of LST sediments. Therefore, according to the development characteristics of the five third-order sequences (Figure 3), two organization patterns of systems tracts can be determined:

Type 1 was dominated by a two-fold structure of systems tracts which contained the TST and the HST. The TST is dominated by a transgressive delta or coastal system; the HST is dominated by a highstand delta; and the tidal flat facies and carbonate platform facies can be developed under a special geomorphic background.

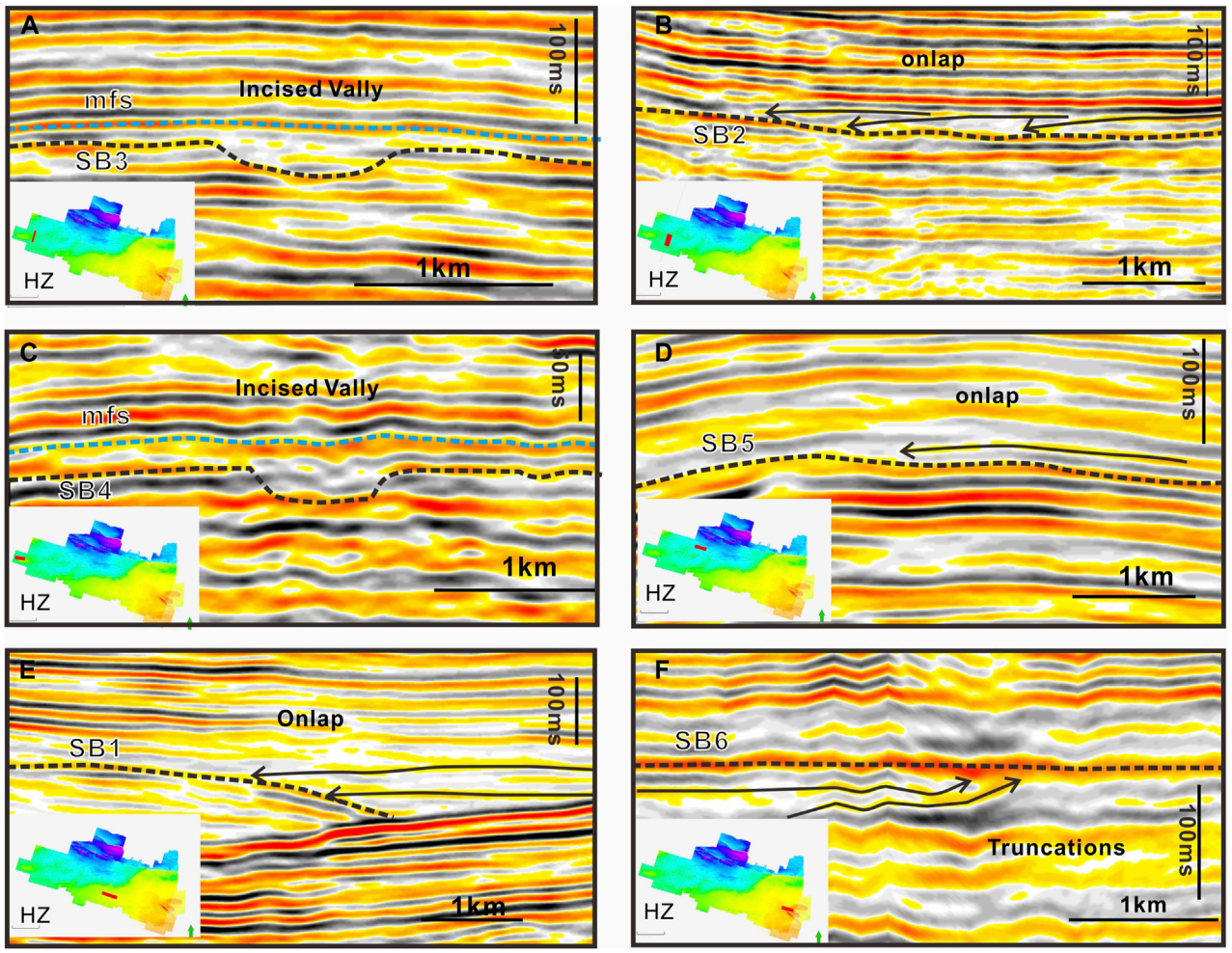

FIGURE 4
(A–F) Seismic responses of typical sequence boundaries recognized in this study.

This type of sequence includes the early SQ1 and SQ2 in the Zhujiang Formation. It reflects that the relative sea level rises and falls slowly and that the sediment supply is sufficient.

Type 2 stratigraphic pattern was featured by the local development of the LST within the low-lying area between the delta front and the carbonate platform. The slope fan and the progradation complex are recognized near the slope or the foot of the slope break zone (Figure 5C). Therefore, the occurrence of LST may be related to the slope break zone.

4.2 Major depositional elements

After the sequence stratigraphic interpretation, the root-mean-square (RMS) attributes of each third-order sequence were extracted to examine the sedimentary system in the study area. This was done by integrating the coring and logging data (Figures 8–11). Through the evolutionary processes, five primary depositional facies associations were identified, along with their correlated subfacies and microfacies.

4.2.1 Deltaic deposits

Deltaic systems are the most prevalent and developing depositional systems in the Zhujiang Formation of the Huizhou Area (Figures 8A, B). In general, four primary subfacies of the deltaic environment can be identified:

4.2.1.1 Upper delta plain

It appears when the main channel begins to branch into a large number of branches (Figures 9A–C). Well log motifs are dominated by staked coarsening-upward cycles. They are characterized by high sand content, and mud is surrounded by sand. The sediment grain size is overall coarse and mainly conglomerate sandstone.

4.2.1.2 Lower delta plain

The sediment primarily consists of medium sand, interbedded with fine sandstones and mudstones (Figure 8). The sorting is generally good or better, and a significant amount of plant debris and mica can be clearly observed (Figure 8). Distributary channels, which form the basic framework of the lower delta plain, typically feature an erosion surface at the bottom. The upper part consists of

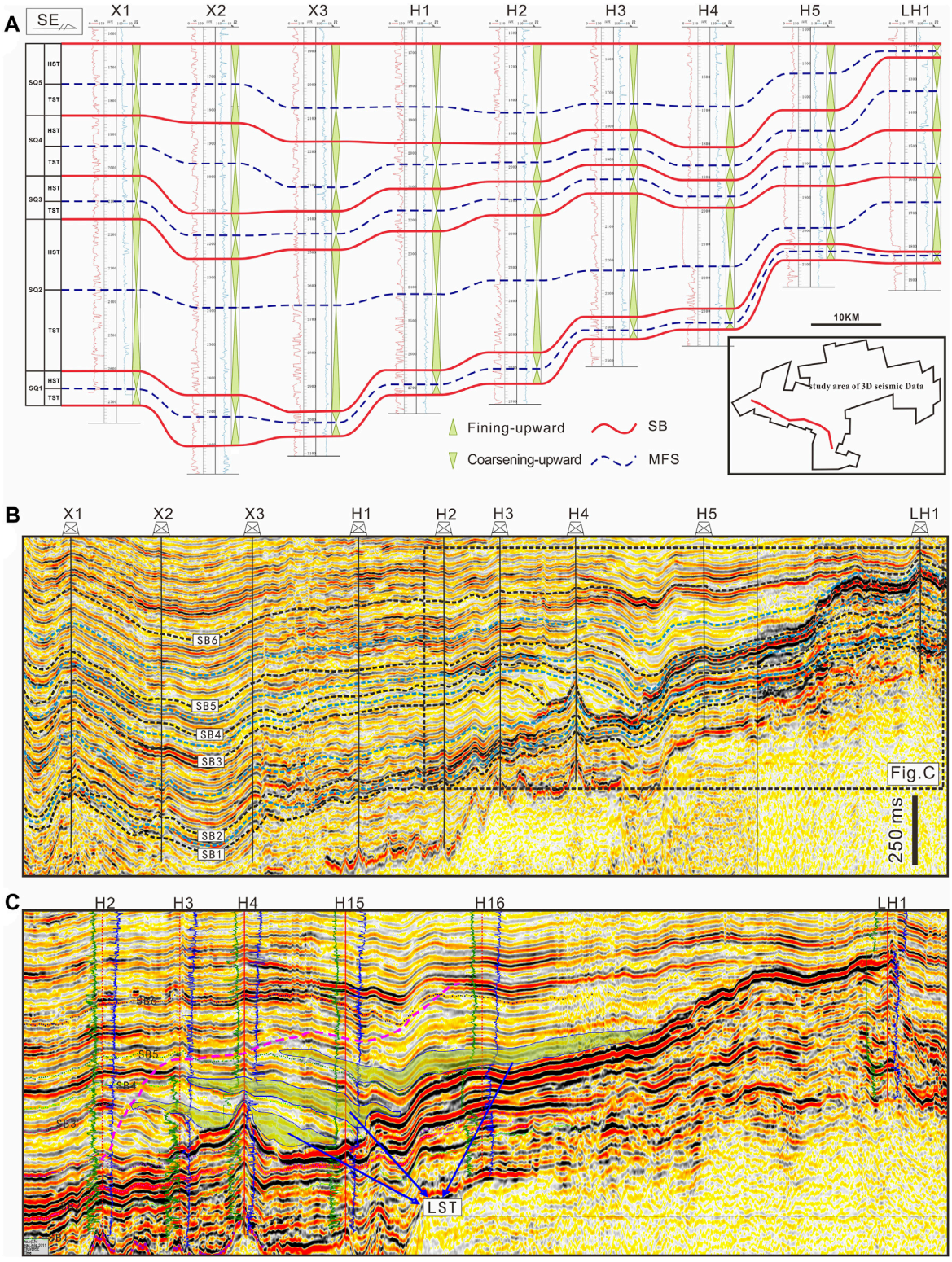

FIGURE 5
NW–SE oriented well log cross-section **(A)** and seismic profile **(B)** showing the major sequences recognized in the south region of the Huizhou Area. **(C)** Note the migration of shoreline positions and the local development of lowstand systems tracts (LSTs).

coarse retention deposits, while the vertical section exhibits an intermittent positive rhythm of coarser materials at the bottom and finer ones at the top (Figure 8A). The cross-section of the sand body is lens-shaped and elongated along the river bed. Interdistributary bay deposits are composed of thin silty-sandstone, sandy-mudstone, and mudstone, with wavy stratifications (Figure 8B). They display relatively high GR values and have slightly serrated well log patterns.

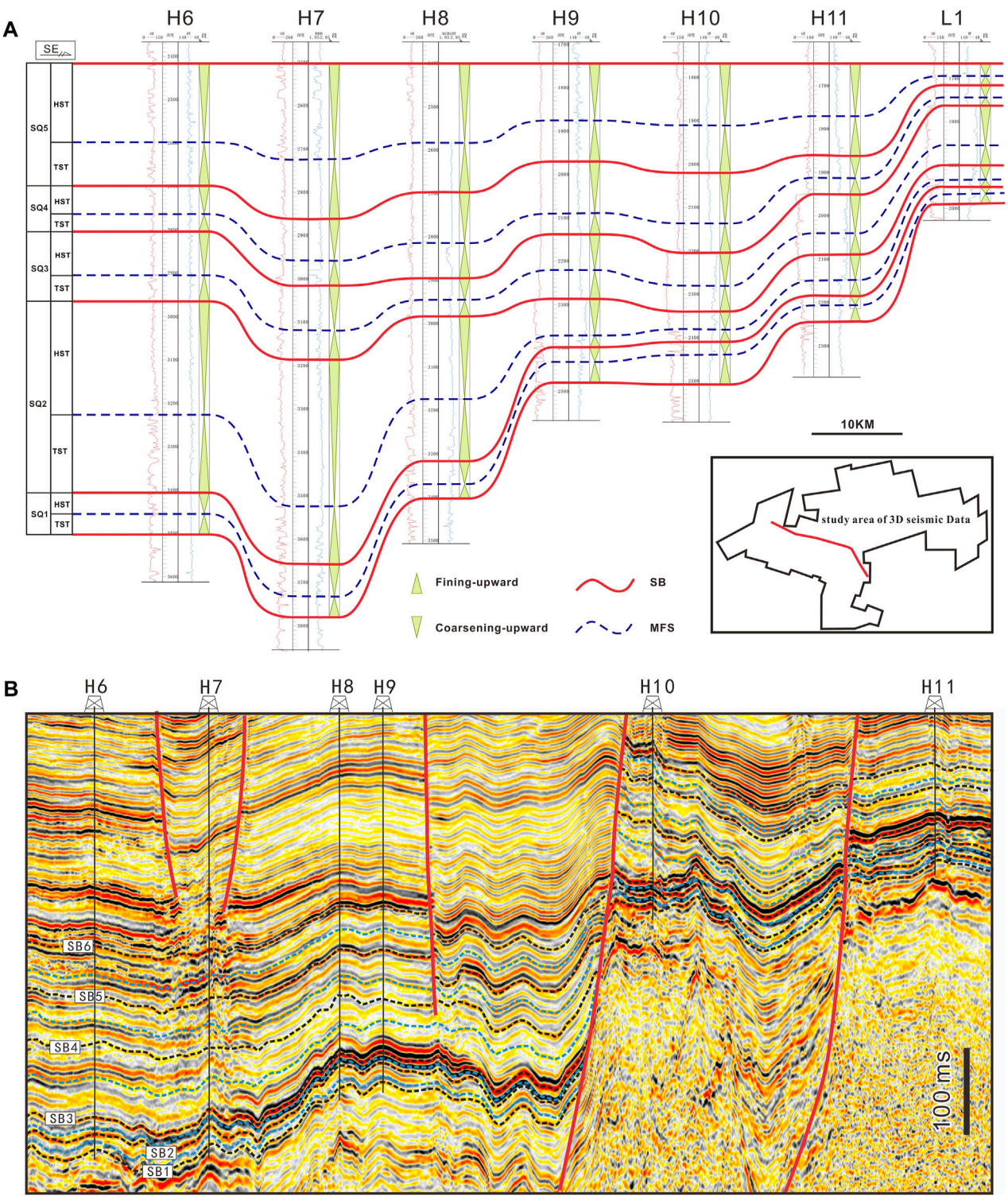

FIGURE 6
NW–SE oriented well log cross-section **(A)** and seismic profile **(B)** showing the major sequences recognized in the north part of the Huizhou Area.

4.2.1.3 Delta front

The delta front represents the underwater part of the delta, which can be further divided into a few microfacies such as subaqueous distributary channels, river mouth bars, and frontal sand sheets. Subaqueous distributary channels are the terminal part of the delta distributary systems (Olariu and Bhattacharya, 2006). The lithology is mainly medium and fine sand. The sedimentary structures are graded beds and parallel stratifications, with typical erosion surfaces at the base (Figure 8). River mouth bars are overall lobe-shaped, and the lithology is mainly fine sandstone. Well log motifs are mainly funnel-shaped,

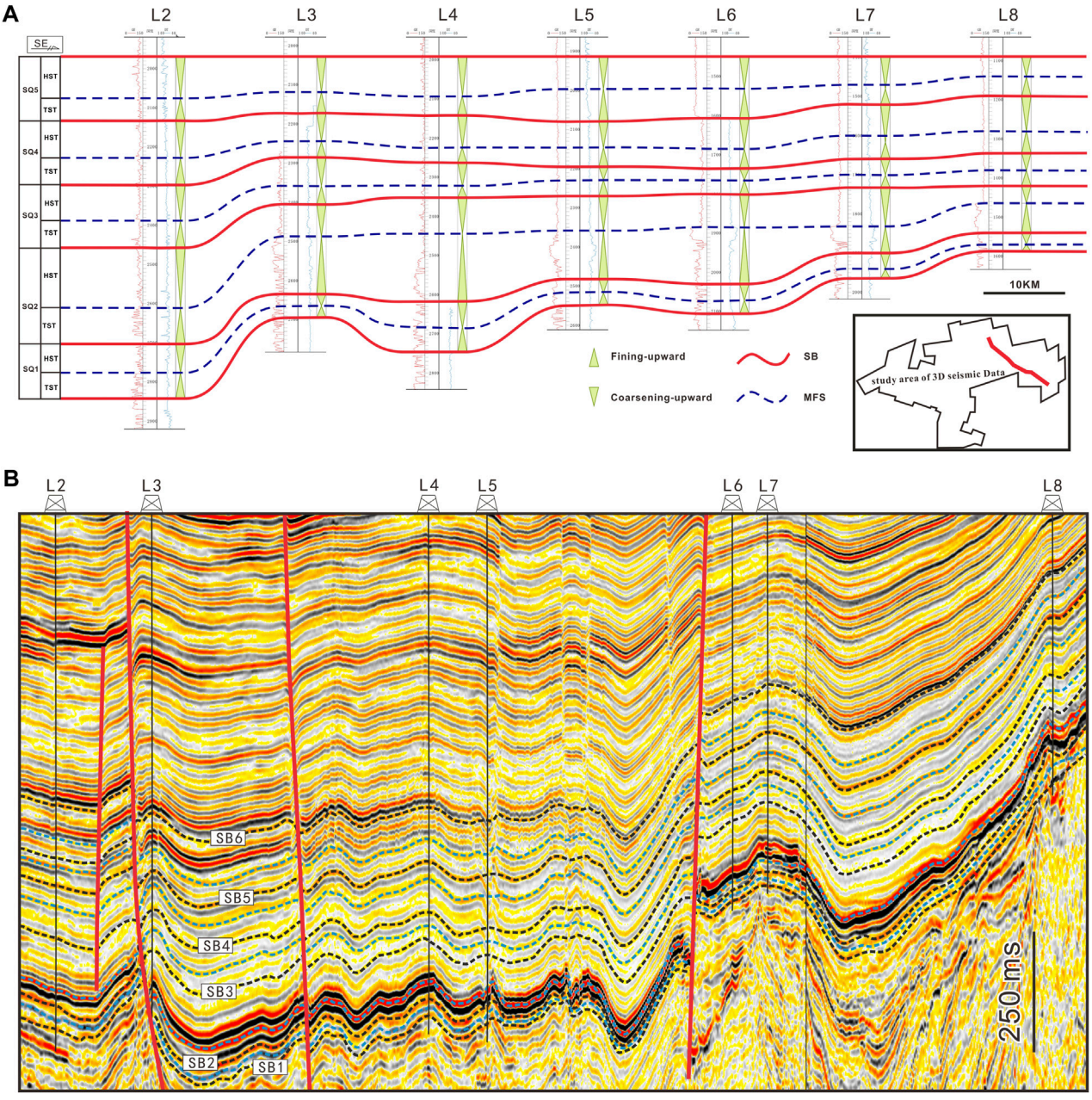

FIGURE 7
NW–SE oriented well log cross-section **(A)** and seismic profile **(B)** showing the major sequences recognized in the Lufeng Area.

finger-shaped, and box-funnel-shaped. They display parallel–subparallel and moderate continuity, with good strong seismic reflection.

4.2.1.4 Pre-delta

The pre-delta subfacies are situated ahead of the delta front and represent the sedimentary portion beneath the wave base. The lithology is primarily composed of dark claystone and silty claystone, with occasional small amounts of fine sand. Authigenic minerals, such as glauconite, can sometimes be observed. Horizontal beddings are frequently developed, and euryhaline fossils are common. These characteristics suggest a quiet depositional environment with low energy, typically found in deeper water settings.

4.2.2 Shoreface

The shoreface association of the Pearl River Delta mainly contain two subfacies: foreshore and nearshore. The foreshore deposits lie between the mean high tide line and the mean low tide line. Based on core observations (Figures 8C–H), it is mainly composed of fine-medium sandstone and mainly massive bedding, which is well sorted and subcircular, with the presence of the swash cross beddings. At the top of the thick layer of sand, we often see erosion cutting and a formed erosional contact. Numerous bioclasts were found, and shell fragments were well-preserved (Figure 8).

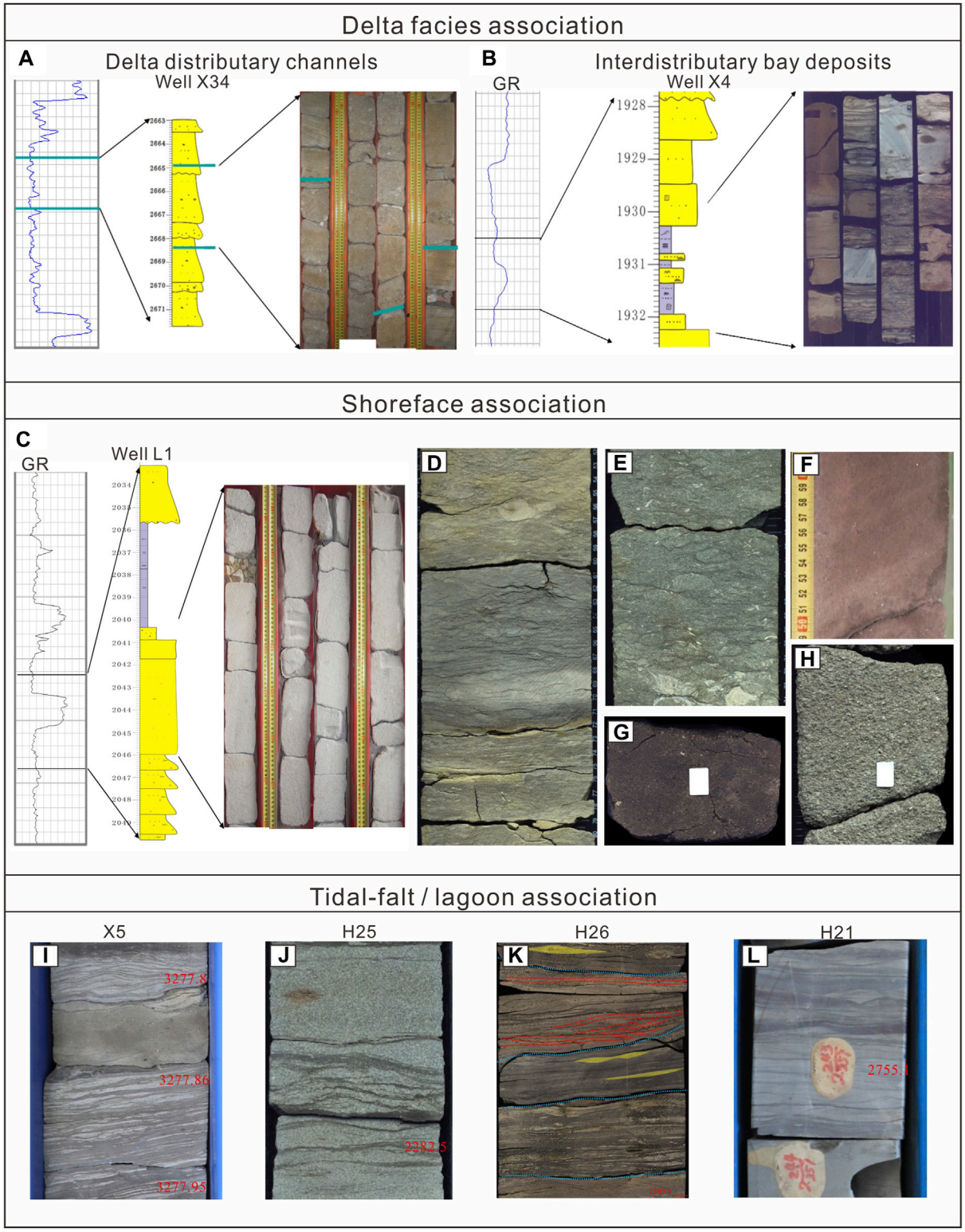

FIGURE 8
(A–C) Well log motifs and core photos of delta distributary channels, interdistributary bays, and shoreface deposits. **(D)** Sedimentary characteristics of foreshore subfacies, featured by dark gray muddy siltstone, with mud interlayers and lenticular cross beddings. **(E)** Lowershore gray dark silty mudstones with pebbles at the base. Note the intense bioturbations and shell fragments. **(F)** Foreshore, brown, and medium sandstones interbedded with mud layers and bioclasts. **(G, H)** Longshore bar deposits, dominated by pebbly to very coarse sandstones, well-sorted, and sometimes oil bearing. **(I–L)** Core photos of tidally influenced delta front deposits. Note the presence of wavy, lenticular, and faster beddings.

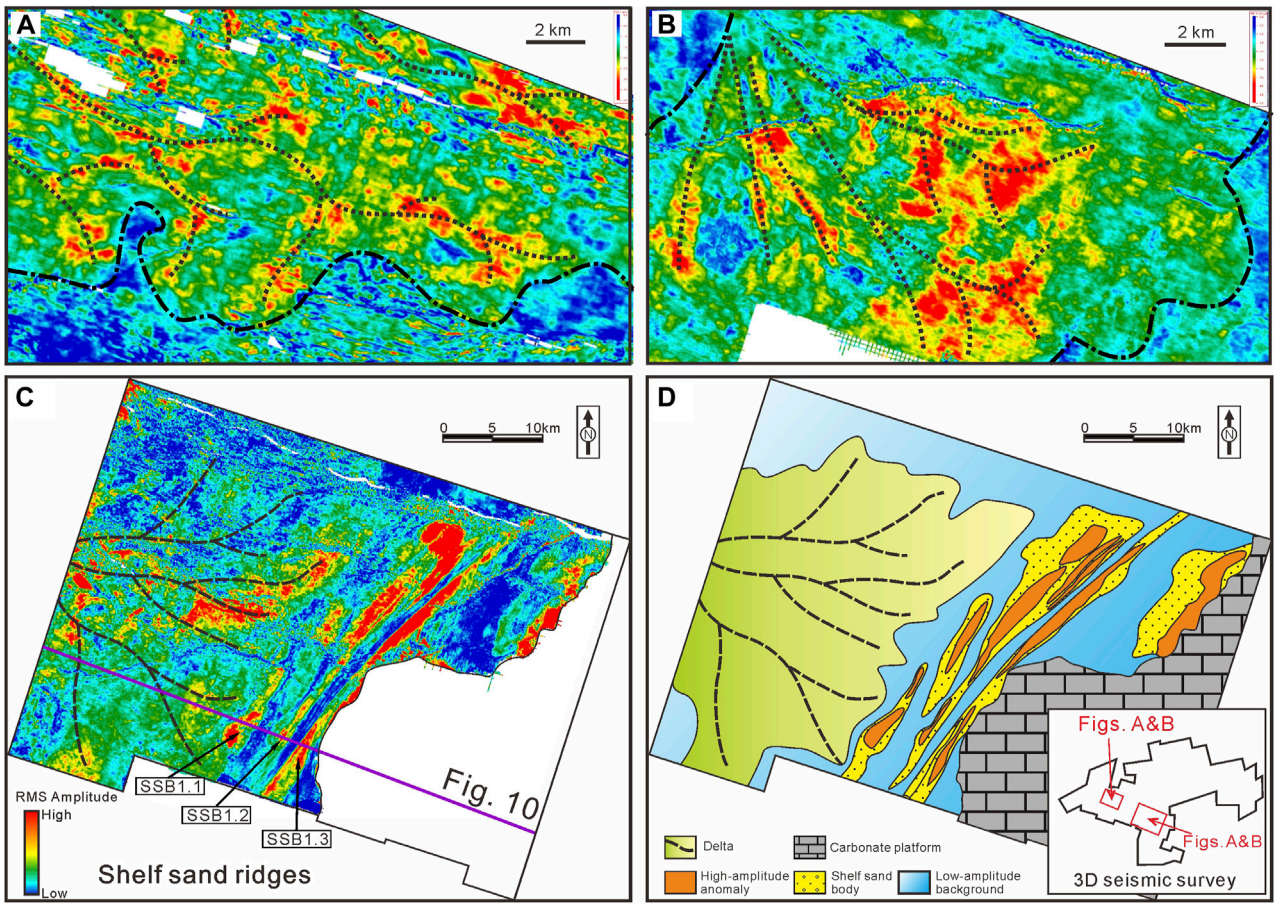

FIGURE 9
(A,B) Extractions of seismic attributes, showing the distribution of deltaic distributary channels within the SQ3 and SQ4, respectively; **(C,D)** Seismic responses and sedimentologic interpretations of shelf sandbodies of the upper SQ2. See panel D for map location.

The nearshore subfacies lies between the mean low tide line and the wave base. Depending on the intensity of hydrodynamic conditions, this subfacies can be further divided into upper nearshore and lower nearshore. The upper shoreface deposits are primarily composed of light brown sandy conglomerates or conglomerate-bearing sandstones, with most gravels being fine-grained. Cross-beddings are prevalent, and the sorting is generally medium (Figure 8C). Well log patterns exhibit coarsening-upward box-shaped motifs with significant grain size variations.

The lower shoreface deposits mainly consist of mudstone, silty mudstone, and argillaceous siltstone, with occasional appearances of light-grey medium to fine sandstone. Massive beedings and parallel stratifications are common, transitioning into lenticular stratifications in the seaward direction. The gamma curve is negative, displays a sharp mouth shape, and is distinctly toothed. It does not show obvious depositional cycles and is primarily composed of silty mudstone (Figure 8C).

4.2.3 Tidal flat and lagoon facies

During the deposition of the Lower Zhujiang Formation, the tidal flat-lagoon sedimentary system primarily developed in the eastern margin of the Dongsha Rise, specifically within the Huizhou Sag. This development was influenced by the combined effects of the confined topography and tidal currents (Figures 8I–L). Vertically, the tidal deposits within the study area are predominantly characterized by tidal flat facies at the base, primarily constituted by quartz-sandstone interbedded with mudstone layers (Figure 8). The quartz-sandstones are clean and moderately sorted. Moving upwards, these transition into lagoon deposits, the lithology of which is dominated by thick mudstone layers interbedded with thin layers of siltstone and dolomite limestone.

4.2.4 Carbonate systems

The carbonate systems within the study area primarily comprise subfacies such as open platforms, platform edges, and platform front slopes. They can be distinctly observed in seismic sections near the Dongsha Rise (Figure 10). The open platform is an environment located behind the platform edge, typically characterized by low energy and stable water conditions. Given the relatively good water circulation and normal salinity, this environment is conducive to life. Conversely, the sedimentary structure undergoes significant changes and contains a substantial amount of lime mud, leading to the formation of various types of limestone (Figure 10).

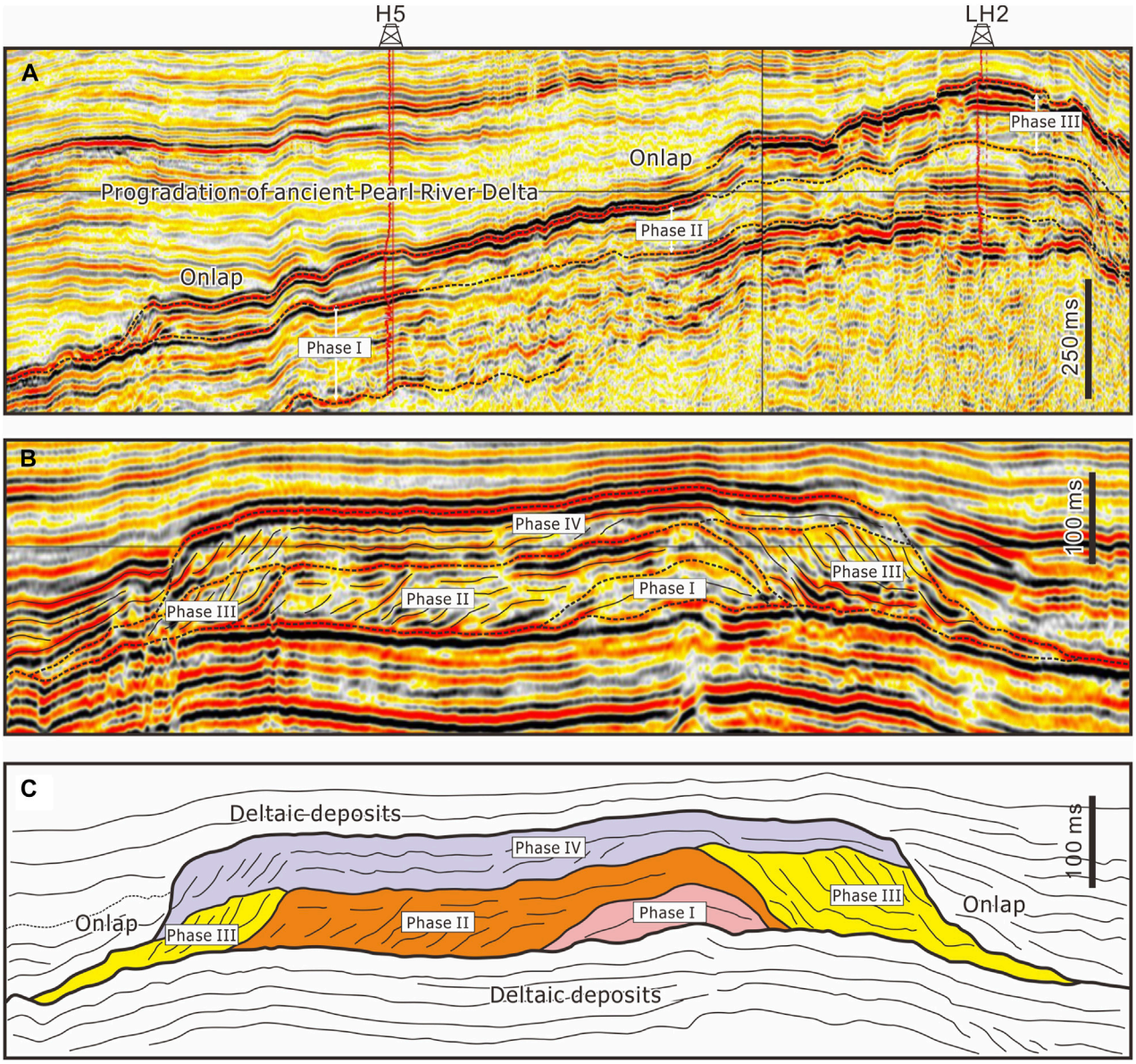

FIGURE 10
Seismic responses of carbonate platforms above the Dongsha Rise. Note that the contracts between carbonate platform and the siliciclastic strata are represented by high-amplitude reflections. **(A)** Seismic profile with well calibration showing the seismic response of three major stages of carbonate platforms; **(B,C)** Seismic profile and stratigraphic interpretation of an typical isolated carbonate platform. See Figure 1 for map location.

The platform edge reef is located near the wave breaking zone of the platform edge. Reef-building organisms mainly consist of coralline algae (red algae), corals, sponges, mosses, and green algae (Figure 11). These are primarily algae and exhibit a twining structure, crust-shell structure, and tuberculous structure. The gamma ray (GR) is low, the curve is box-shaped and displays micro-dentate characteristics, and the amplitude change is consistent.

Platform edge shoals are generally found on the edge of the platform reef to the side of the platform, representing a shelf transition. These shoals have strong hydrodynamic conditions, with bioclastic shoals being developed and low gypsum content. Under suitable conditions, reef bodies can develop and form, resulting in alternating interbeds of reef and beach deposits (Figure 10).

4.2.5 Shallow marine facies

The shallow marine system represents one of the most distal environments within the study area, with the sandbodies being mostly shore-parallel (Figure 9D). The hydrodynamic conditions of the continental shelf are complex and diverse, including ocean currents, waves, tidal currents, and density currents (Zhuo et al., 2014; He et al., 2017). These processes tend to act within various water depths. In the inner-shelf region, the presence of ripple cross beddings indicates the influence of tide or wave actions. Other than normal wave or tide actions, storms also influence the shallow

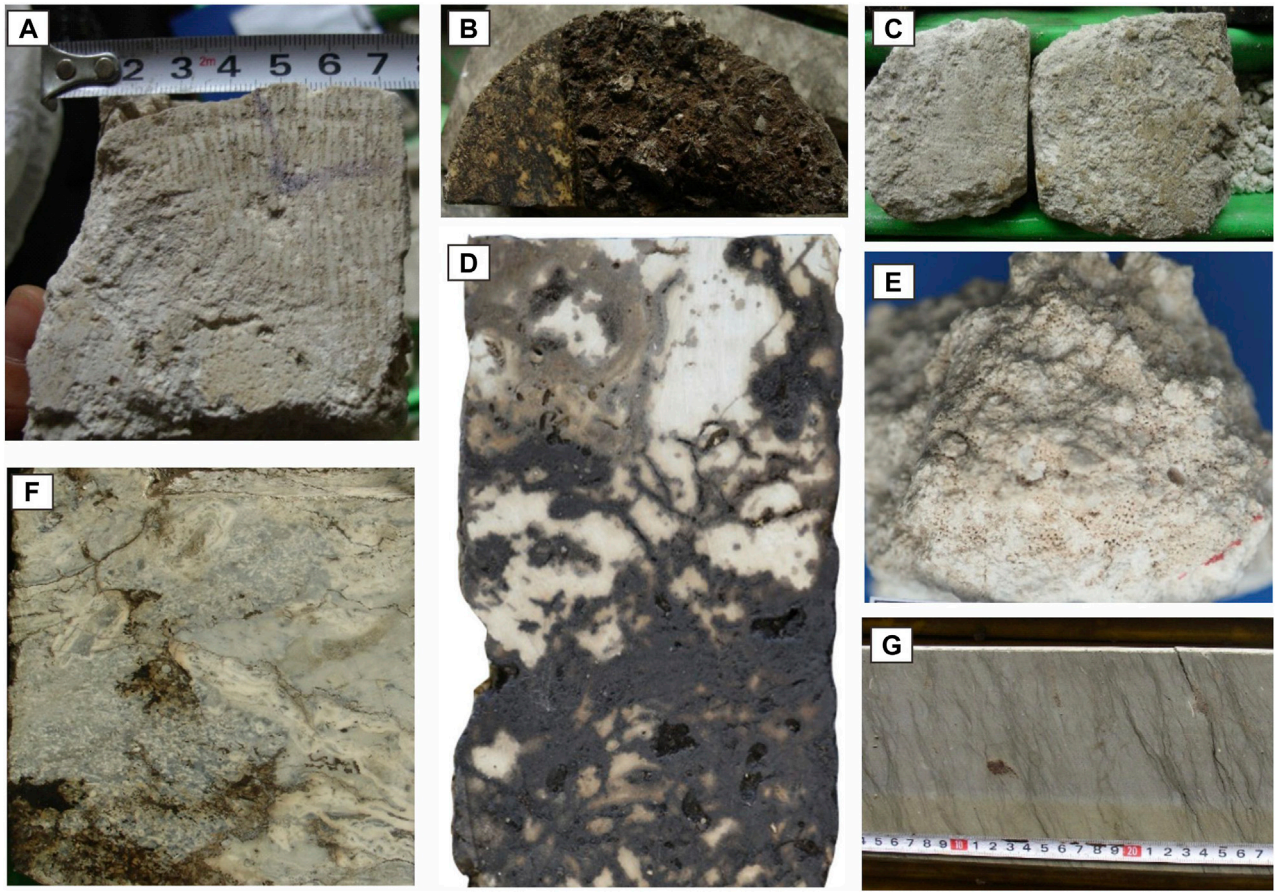

FIGURE 11
Lithology of carbonate deposits revealed by core photos from various wells that intersected the carbonate platform. **(A)** Reef facies deposits, mainly framework limestones; **(B)** Fore-reef slope facies, dominated by slumped breccia; **(C)** Shoal of platform margin, dominated by gray to white algal limestones; **(D)** Reef of platform margin, mainly bafflestones with algal agglomerates and dissolved pores; **(E)** Reef of platform margin, dominated by reef framework limestones; **(G)** Open platform lagoon deposits, dominated by gray biomicrite with mud drapes; **(F)** Organic reef and shoal complex, featured by the presence of algal agglomerates and dissolved pores.

marine deposits, as indicated by the block cross beddings instead of ripple cross beddings.

Isolated shelf sandbodies are perpendicular to the shoreline and parallel to the direction of the tidal or longshore currents (Figure 9B). Because of the long-term reworking of marine processes, the content of sand is relatively high, and the shelf sandbodies tend to be composed of clean and well-sorted sandstones, which are encased in shelf mudstones. The GR curve corresponding to the shelf mud in the shallow sea has an abnormally low amplitude, reflecting relatively pure thick mudstone deposition under the condition of still water.

5 Discussion

5.1 Depositional evolution

During the deposition of the Zhujiang Formation, three major depositional stages were identified for the Zhujiang Formation during 21–16.5 Ma (Figure 12).

5.1.1 Stage 1: Dominance of deltaic and shoreface systems

Stage 1 primarily involves the deposition of the SQ1 sequence. During this stage, seawater started to infiltrate the Zhu I Depression, resulting in the formation of a relatively thin transition sequence that had a high sand content (Figure 12A). The deposition of the Zhuhai Formation essentially covered the previously existing multi-sag topography, leading to the creation of a gentle shelf environment, particularly evident since the deposition of the Zhujiang Formation. At the same time, the second jump of the mid-ocean ridge caused the Zhu II Depression to significantly subside and the seawater to encroach to the Zhu I Depression. During this period, the ancient Pearl River Delta and the Hanjiang Delta both advanced from the north or west side of the study area, forming a large delta cluster. In front of these two delta systems, shallow marine depositional systems developed due to the insufficient input of continental clastic material. Most of the Dongsha Rise remained exposed, but its function as a sediment source significantly diminished. Instead, the sedimentary systems of the shoreland and tidal flat-lagoon around the uplifts replaced it, rather than the typical delta systems.

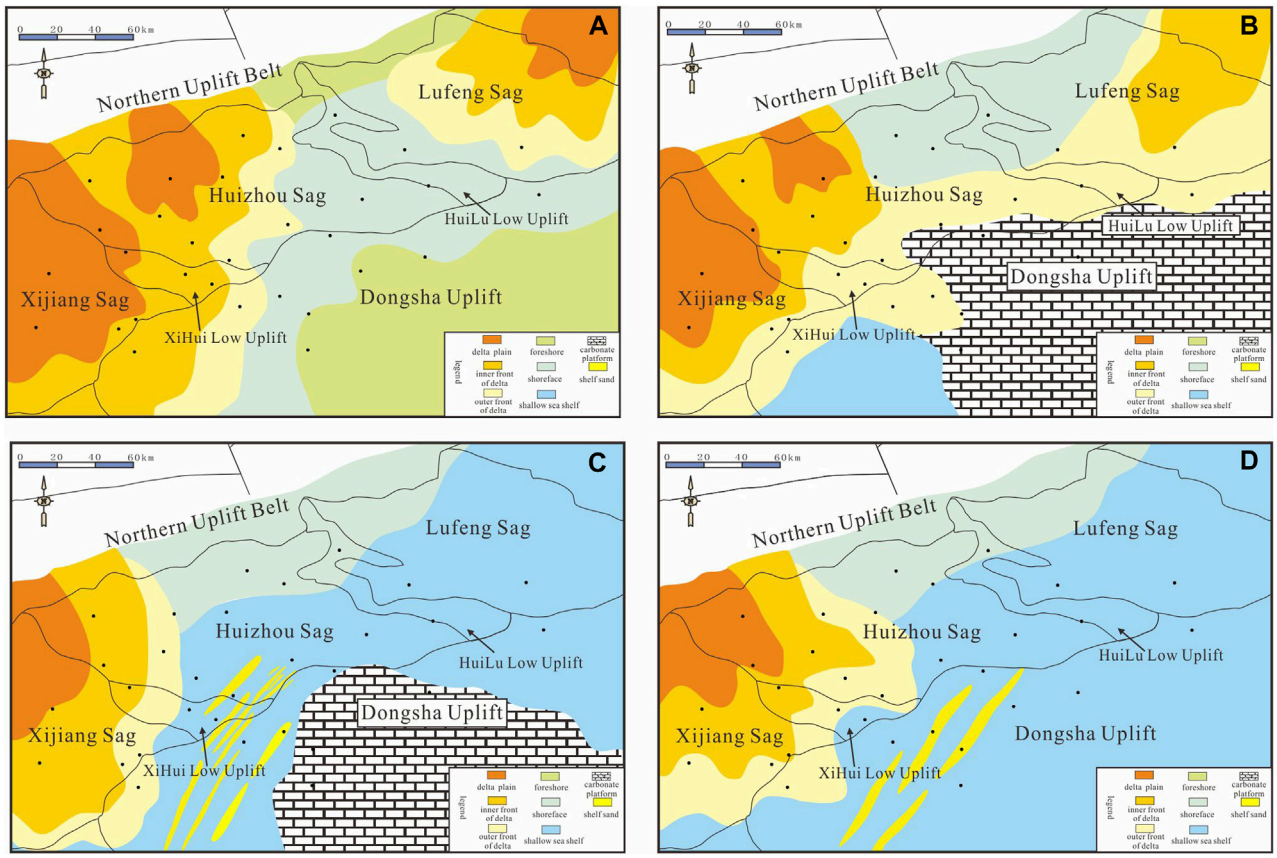

FIGURE 12
Reconstruction of paleogeography during the deposition of the Zhujiang Formation within the study area. **(A)** The depositional system was dominated by deltaic and shore facies (Stage 1). **(B)** The carbonate system began to prevail (Stage 2). **(C)** The study area was jointly influenced by deltaic and carbonate systems, within minor shore-parallel sand ribbons (Stage 3). **(D)** The deltaic and shallow marine systems dominated (Stage 4).

5.1.2 Stage 2: Interactive development of deltaic and carbonate systems

Stage 2 encompasses three sequences, namely, SQ4, SQ3, and SQ2. The most prominent characteristic of Stage 2 is the interplay between deltaic and carbonate deposits. As depicted in Figure 12B, the SQ2 sequence underwent the most significant transgression after the Pearl River Mouth Basin entered the comprehensive depression stage, leading to the formation of the largest floating surface MFS18.5 in the Pearl River Mouth Basin. This resulted in the largest transgression systems tract and highstand systems tract (HST) in the Pearl River Mouth Basin. During this period, the ancient Pearl River Delta receded to the northwest, but it remained the primary sedimentary system in the study area. The ancient Hanjiang Delta also retreated from the study area and was only present in the north of the Lufeng Depression. The exposed area of the Dongsha Rise dramatically decreased, and thin layers of limestone began to develop where the shoreland and tidal flat-lagoon sedimentary systems were previously established, forming typical carbonate slope deposits. Towards the end of the transgression, the accumulation of carbonate rocks intensified, resulting in a massive carbonate platform. Importantly, by the end of the transgressive systems tract (TST), although the Dongsha Rise was still dominated by carbonate platform facies, the platform's area started to decline due to the advancement of the ancient Pearl River Delta.

The following two third-order sequences, SQ3 and SQ4, largely mirror the sedimentary facies distribution of the SQ2 sequence (Figure 12C). However, due to the evolution of the carbonate platform, a restricted trough was formed between the shoreline break and the carbonate platform in the early stage. This led to the emergence of a local lowstand systems tract (LST) above the sequence interface. Influenced by the confined trough, several shelf sand ridges were constructed in front of the ancient Pearl River Delta (Figure 12C).

5.1.3 Stage 3: Prevalence of deltaic and shallow marine environments

During Stage 3, primarily characterized by the SQ5 sequence (Figure 12D), all carbonate platforms started to submerge, becoming overlaid by shallow marine deposits. The entire study area was dominated by delta and shallow marine shelf facies, with the shoreland facies persisting in the northern region. With the barrier effect of the carbonate platform no longer present, the delta lobes extended further during the late phase of the HST, culminating in the maximum marine regression of the secondary cycle within the Zhujiang Formation.

5.2 Preservation of lowstand deposits

A thorough analysis of the sequence stratigraphy reveals two distinct systems tract organization patterns, contingent upon the presence or absence of the LST. Generally, the lower two sequences, SQ1 and SQ2, do not display prominent LSTs, while the upper three sequences clearly exhibit local LSTs (Figure 5). The emergence of the LST around 18 Ma is speculated to be more than coincidental; it is likely closely tied to the gradual increase in sediment accommodation, potentially influenced by a complex array of driving factors. Around 23.8 Ma, concurrent with the onset of the Baiyun Movement, the shelf edge markedly shifted northward, creating favorable conditions for the growth of the carbonate platforms in the vicinity of the Dongsha region (Pang et al., 2007a; Pang et al., 2007b; Liu et al., 2011; Zhuo et al., 2019).

In the early stages (prior to 18 Ma), the influx of terrigenous sediments into the shelf area was minimal. As a result, the typical clinoforms of the Pearl River Delta were not yet fully formed, exhibiting a relatively low height and slope gradient. However, around 18 Ma, with the onset of SQ2 formation, the carbonate platform on the Dongsha Rise underwent significant development, forming a distinct, elevated structure at the forefront of the study area. Concurrently, the increasing height and gradient of the Pearl River Delta's clinoforms led to the emergence of a depositional break. A structural low was also created between the delta front and the carbonate platform, which we believe played a crucial role in the sedimentation and preservation of the LSTs within the upper three depositional sequences. As depicted in Figure 5, the LST deposits clearly onlap onto the pre-existing highstand successions, while simultaneously downlapping the carbonate platform of the Dongsha Rise. As the local structural lows between the delta and the platform gradually filled in, the scale of the LST rapidly diminished, and the LST completely vanished after the deposition of the SQ5. Subsequently, the slope break of the sedimentary shoreline traversed the Dongsha Rise, aligning with the shelf slope break during the LST.

5.3 Confined topography and hydrodynamic process

During the deposition of the Zhujiang Formation, the development of the shelf sand ridges have been recognized in the study area (Figure 9B; Figures 13, 14). Shelf sand ridges are often isolated in shelf fine-grained sediments, forming the potential oil and gas reservoir sand bodies (Zhuo et al., 2014). Initially, researchers interpreted these isolated sand bodies as transgressive shelf sand ridges. Along with the advancement of sequence stratigraphy, some workers began to doubt the transgressive origin and reinterpreted them as incised valley fills or forced regressive deposits (Walker and Bergman, 1993; Bergman, 1994). Recently, various scholars gradually hypothesize that the development of these isolated shelf sandbodies cannot be explained with a single model and is more likely controlled by interactive processes (Posamentier, 2002; Suter, 2006; Zhuo et al., 2014).

Based on the established sequence stratigraphic framework, we have determined that the formation of the shelf sand ridges within the study area commenced around 18 million years ago, subsequent to the deposition of the SQ3 (Figure 13). In addition, no obvious shelf sand ridges were found in the early stage of the SQ1 and SQ2. As illustrated by the RMS amplitude extractions, the variation in the width and narrowness of the shelf sand ridges exhibits clear bidirectional patterns revealed by seismic attributes, i.e., widening to both NE and SW directions (Figure 9). This indicates that its formation may be controlled by bidirectional paleocurrents. Certain sedimentary structures revealed by core data, such as mud drapes, also indicated that the shelf sand ridges were formed not by unidirectional paleocurrents but by bidirectional ones, among which the shelf tidal current may be the most important. The shelf sand ridges developed in the Zhujiang Formation of the study area are clearly different from the shelf sand ridges in the open-shelf environment reported by Zhuo et al. (2014); these shelf sand ridges were mainly controlled by unidirectional, permanent, or semi-permanent shelf currents.

In this study, we attribute the onset and cease of the shelf sand ridges to the interaction between local confined topography and paleo-hydrodynamic conditions. Commonly, the strength of ocean currents can be significantly enhanced during marine transgression (Catuneanu, 2006). One of the most significant marine transgression took place at ca. 18 Ma and reached the maximum at ca. 18.5 Ma. As a result, the hydrodynamic force of the ocean substantially intensified during this transgressive event. In the late stage of the SQ2 sequence deposition, around 18 million years ago, a large-scale transgression transpired in the study area, peaking at approximately 18.5 million years ago. Moreover, when the ocean current flowed over the constricted topography formed by the delta and the Dongsha Platform, its strength was further amplified.

Based on the analysis above, we can reconstruct evolution history of the shelf sedimentary systems (Figure 14): first, along with the transgression that occurred in the northern South China Sea at ca. 18 Ma, the delta gradually prograded to the west of the Dongsha Rise and formed a restricted continental shelf trough to the platform. This enhanced the strength of the shelf tidal currents that flow through the trough under the seasonal wind field; then, the sand bodies at the front of the delta were severely reworked to form mounded shelf sand ridges encased within the shelf mud deposits (Anell et al., 2020).

5.4 Implications for tectonics and provenance changes

Spanning ca. 23–16.5 Ma, the stratigraphy and sedimentation of the Zhujiang Formation recorded the final stage of seafloor spreading and tectonic evolution of the South China Sea, from the southward jump to the dying of the spreading center (Sun et al., 2009; Li et al., 2013). The ridge jump at 20.03 Ma was manifested as the strong subsidence of the Baiyun Sag in the deep water of the South China Sea, while the shelf edge significantly migrated from the Southern Uplift Belt to the northern slope of the Baiyun Sag. Therefore, the Zhu I Depression, where the Huizhou Sag is located, formed a consistent shallow marine environment ever since. In response to the spreading ridge jump, a gradual marine transgression was recorded in the sedimentation of the Zhujiang Formation, evidenced by the fining-upward sequence stacking patterns (Figures 4–6). Also influenced by marine transgression,

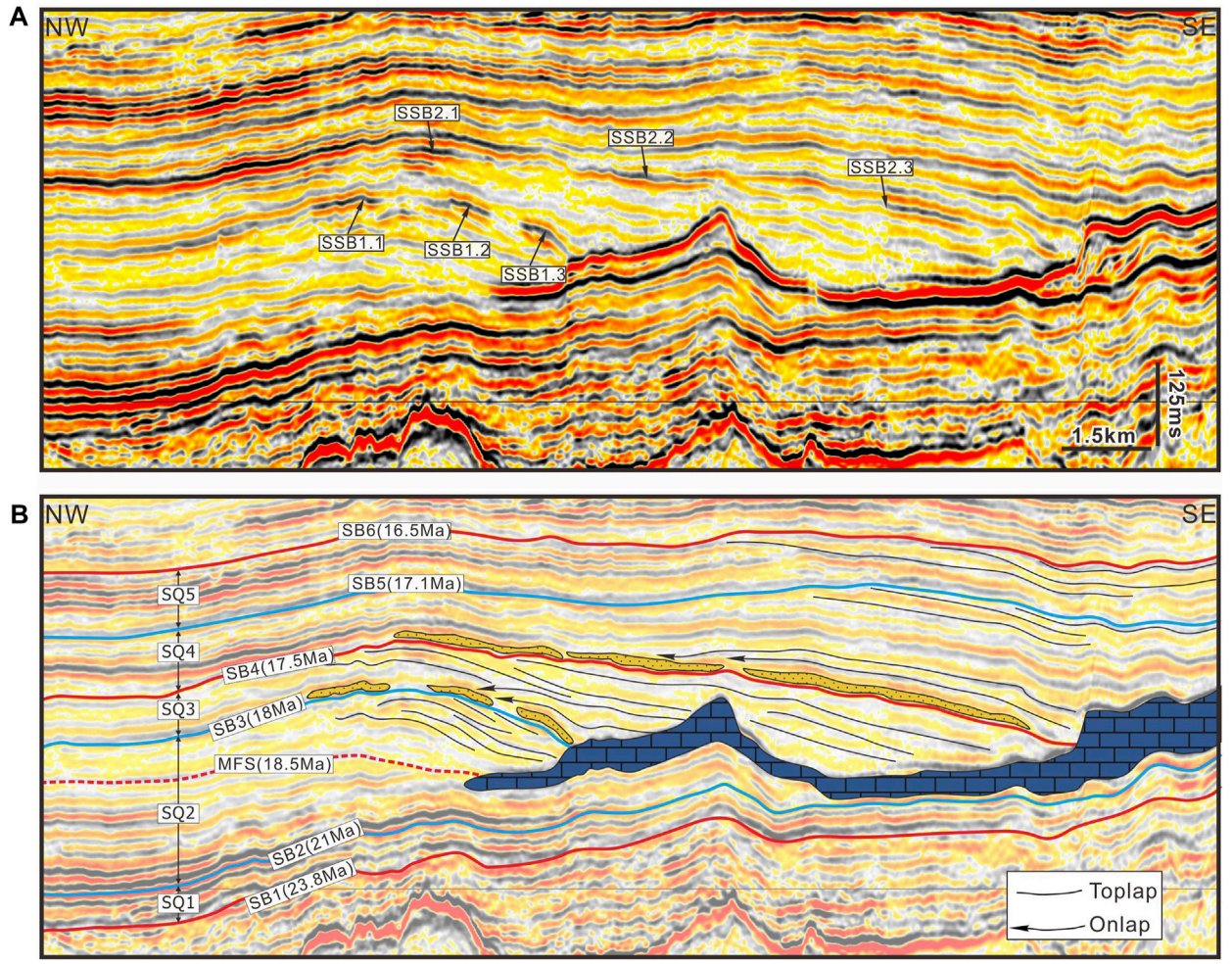

FIGURE 13
Seismic section **(A)** and associated interpretation **(B)** showing the characteristics of isolated shelf sand ridges that developed within the study area. See Figure 9 for line location.

carbonate platforms began to grow atop the structural highs of the Dongsha Rise.

At ca. 19.1 Ma, the first large-scale transgression in the Pearl River Mouth Basin occurred, forming a regional marine mudstone covering the whole Zhu I Depression, which is also the period that carbonate in the Dongsha Rise started large-scale development and formed the first set of good reservoir-seal assemblage of Neogene in the Pearl River Mouth Basin. Other than the tectonics of the South China Sea, the stratigraphy and sedimentation of the Zhujiang Formation also recorded a provenance alteration since ca. 23 Ma, along with the Baiyun Movement (Shao et al., 2005; Pang et al., 2007b). At this time, affected by the uplift of the Himalayan Mountain Belt, the hinterland of the ancestral Pearl River expanded to the west to the carbonate provenance system of the Yungui Plateau at the eastern foot of the Tibetan Plateau. This resulted in a dramatic change in the source sediment texture, i.e., from sand-rich to mud-rich. This sudden change in source area was also recorded in the sedimentation of the Huizhou Sag. In Huizhou Area, the sediments in the Upper Zhujiang Formation have relatively finer grain size and lower sand percentage, compared with the Lower Zhujiang Formation.

5.5 Significance for hydrocarbon exploration

The wide variety of sedimentary facies and the cyclic progradation/retrogradation of the ancient Pearl River Delta system resulted in favorable conditions for the development of various types of sand bodies and lithologic traps in the Huizhou Area, which has been proved by a series of hydrocarbon activities (Figure 15; also see Chen et al., 2012). Different types of sand bodies have different development positions, distribution rules, and pinching-out characteristics.

5.5.1 Lithologic traps

In the study area, the sand bodies near the sequence boundaries have favorable conditions to form lithologic traps (Figure 15). During the deposition of the Zhujiang Formation, the Huizhou Area was in a relatively wide and slow continental shelf environment, and the shoreline migration was very sensitive to the changes in the relative sea level, forming stacked deltaic or shoreface sand bodies. The mudstone developed during the transgression can act as a regional seal for the sandstone near the sequence boundary to form lithologic traps. The types of lithologic traps formed near the sequence boundaries

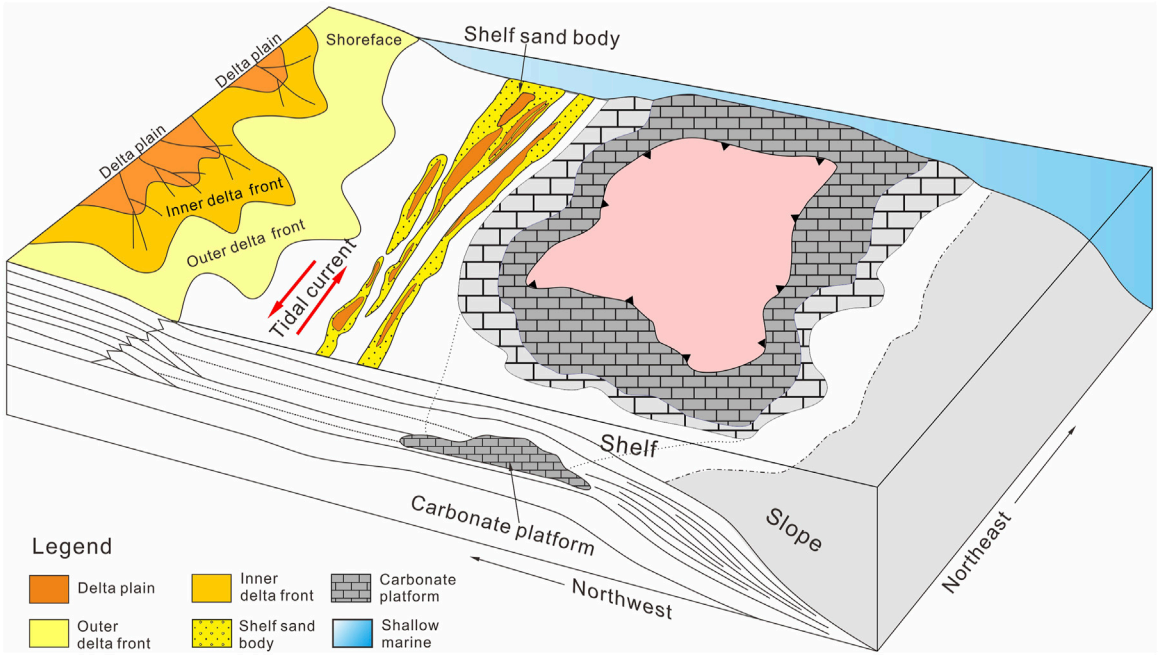

FIGURE 14
Depositional model for the interactive sedimentation of the Miocene Pearl River Delta system and the carbonate platforms.

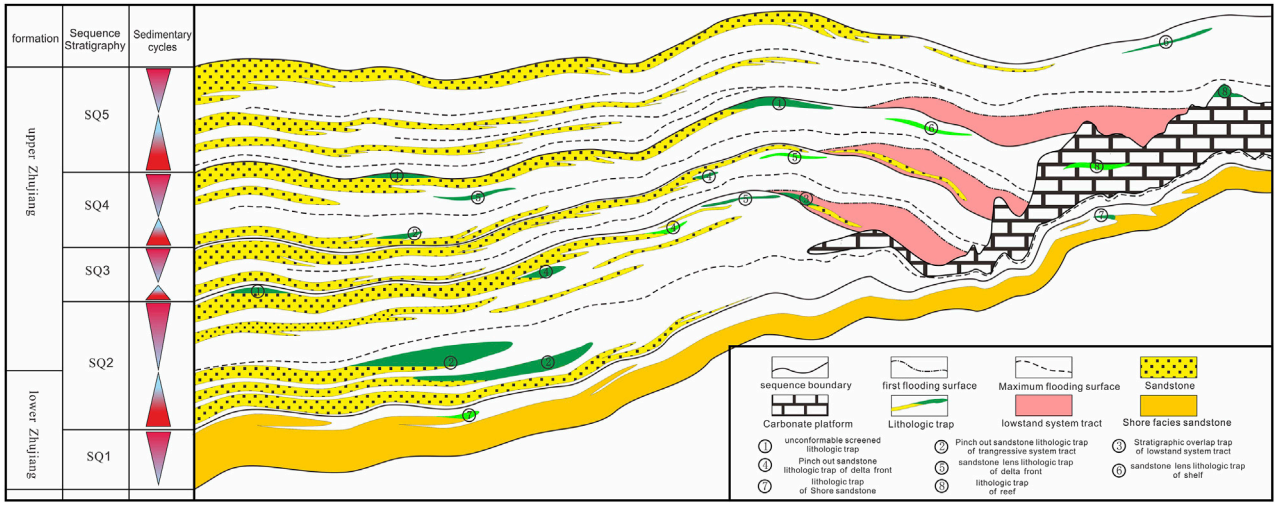

FIGURE 15
Model for the development of stratigraphic and lithologic traps within the Zhujiang Formation in the Huizhou Area, northern South China Sea.

mainly include HST sand pinch out traps below the sequence boundary, LST stratigraphic traps, and TST sand pinch out traps above the sequence interface. In the study area, a large number of hydrocarbon discoveries have been made near the sequence boundaries, such as the NSB21, NSB18, NSB17.5, and NSB17.1.

5.5.2 Carbonate traps

During certain periods of sea-level lowstand (18, 17.5, and 17.1 Ma), carbonate platforms may have been exposed, leading to erosion or freshwater leaching. This exposure resulted in the development of secondary pores in the carbonate rocks near the sequence boundary, forming high-quality reservoirs. As sea levels rose, newly formed carbonates served as a cap layer for the secondary pore beneath the sequence boundaries, thereby creating carbonate lithologic traps. In the final stage of carbonate development, the top layer was directly overlaid by mudstone, providing even better capping conditions.

6 Conclusion

Utilizing a merged 3D seismic volume and over 100 industrial boreholes, this study presents a study on the stratigraphic-sedimentary evolution of a mixed siliciclastic-carbonate system in the Huizhou Sag of the Pearl River Mouth Basin, northern South China Sea shelf. For the Zhujiang Formation which is the interval of interest, we identified five third-order sequences, which collectively form a larger second-order sequence. Based on the development level of the LST deposits, two fundamental sequence stratigraphic architectures were identified. As a comprehensive response to the growth of deltaic clinoforms and the protection of the Dongsha Platform, LST started to develop in the upper three sequences.

Within the study area, five primary sedimentary facies were developed, namely, the delta, shoreface, tidal flat/lagoon, and carbonate platform. We also reconstructed the interactive evolution of siliciclastic and carbonate deposition, considering sediment supply, sea-level fluctuation, hydrodynamic processes, and local paleotopography. The Huizhou Sag likely experienced a succession of delta-shore, delta-shore-tidal-lagoon, delta-shore-carbonate, and delta-shore-shallow marine systems based on sedimentation characteristics. The deposition of the Zhujiang Formation in the Huizhou Area was time-equivalent with the spreading process after the ridge jump of the South China Sea (23–16.5 Ma), providing valuable insights into sea level, provenance, and tectonic history. Furthermore, the ancient Pearl River Delta system provided numerous types of sand bodies as well as hydrocarbon traps. In general, the sandbodies near the sequence boundaries tend to be easily sealed by fine-grained deposits that formed during marine transgression.

Data availability statement

The original contributions presented in the study are included in the article/Supplementary Material, further inquiries can be directed to the corresponding author.

Author contributions

WC: original draft and data interpretation. HZ: conception, original draft, and data interpretation. JL and GP: methodology and editing; ZW, PJ, and JY: interpretation of core, well-log, and seismic data. ZW: figure preparation, reviewing, and editing. All authors contributed to the article and approved the submitted version.

Funding

This study was funded by the Natural Science Foundation of Guangdong Province (grant No. 2019A1515010786), Project supported by Innovation Group Project of Southern Marine Science and Engineering Guangdong Laboratory (Zhuhai) (grant No.311020003/311021004), National Natural Science Foundation of China (grant No. 41706050), National Major Science and Technology Project during the 13th Five Year Plan ("Exploration Frontiers and Key technologies of the Eastern South China Sea", grant No. 2016ZX05024-004).

Acknowledgments

We want to thank CNOOC Shenzhen Limited for the permission to publish the results. Additionally, our sincere thanks go to Dr. Jiayuan Du and Jin Feng for their significant help during the preparation of this paper. The insightful comments from editor Prof. Lawrence Tanner, Dr. Kei Ogata, and two reviewers have greatly improved the final quality of this paper, and we are deeply grateful for their contributions.

Conflict of interest

Authors WC, JL, GP, ZW, PJ, and JY were employed by Shenzhen Branch of CNOOC Limited.

The remaining authors declare that the research was conducted in the absence of any commercial or financial relationships that could be construed as a potential conflict of interest.

Publisher's note

References

Anell, I., Zuchuat, V., Röhnert, A. D., Smyrak-Sikora, A., Buckley, S. J., Lord, G. S., et al. (2020). Tidal amplification and along-strike process variability in a mixed-energy paralic system prograding onto a low accommodation shelf, Edgeøya, Svalbard. *Basin Res.* 33, 478–512. doi:10.1111/bre.12482

Bergman, K. M. (1994). Shannon sandstone in Hartzog Draw-Heldt Draw fields (Cretaceous, Wyoming, USA) reinterpreted as lowstand shoreface deposits. *J. Sediment. Res.* 64, 184–201. doi:10.1306/D4267F87-2B26-11D7-8648000102C1865D

Catuneanu, O. (2006). *Principles of sequence stratigraphy*. Amsterdam: Elsevier.

Catuneanu, O., Abreu, V., Bhattacharya, J. P., Blum, M. D., Dalrymple, R. W., Eriksson, P. G., et al. (2009). Towards the standardization of sequence stratigraphy. *Earth-Science Rev.* 92, 1–33. doi:10.1016/j.earscirev.2008.10.003

Chen, C., Shi, H., and Xu, S. (2003). *Hydrocarbon reservoir forming conditions of tertiary in Pearl River Mouth basin (eastern)*. Beijing: Science Press.

Chen, W., Du, J., Long, G., Chen, S., and Li, X. (2012). Factors controlling sandbody development and models of stratigraphic-lithologic traps of Zhujiang Formation in Huizhou area, Pearl River Mouth basin. *Oil Gas Geol.* 33 (3), 449–458. doi:10.11743/ogg20120315

Chen, W., Shi, H., Du, J., and He, M. (2016). Formation conditions and development model of stratigraphic-lithologic traps in shelf break zone, Pearl River Mouth Basin: zhujing Formation as an example. *Petroleum Geol. Exp.* 38 (5), 619–627. doi:10.11781/sysydz201605619

Dong, W., Lin, C., Qin, C., Xie, L., Yang, X., Cui, L., et al. (2008). High resolution sequence framework, depositional attern and litho-stratigraphic traps of Hanjiang Formation in panyu uplift, Pearl River Mouth basin. *Geoscience* 22 (5), 794–802.

Du, J., Shi, H., Ding, L., Chen, W., Luo, M., and Long, G. (2014). An analysis of favorable exploration areas for stratigraphic-lithologic hydrocarbon accumulation in the eastern Pearl River Mouth basin. *China Offshore Oil Gas* 26 (3), 30–36.

Gong, Z., Li, S., Xie, T., Zhang, Q., Xu, S., Xia, K., et al. (1997). *Continental margin basin analysis and hydrocarbon accumulation of the northern South China sea*. Beijing: Science Press.

Haq, B. U., Hardenbol, J., and Vail, P. R. (1987). Chronology of fluctuating sea levels since the Triassic. *Science* 235, 1156–1167. doi:10.1126/science.235.4793.1156

He, M., Zhuo, H., Chen, W., Wang, Y., Du, J., Liu, L., et al. (2017). Sequence stratigraphy and depositional architecture of the Pearl River Delta system, northern South China Sea: an interactive response to sea level, tectonics and paleoceanography. *Mar. Petroleum Geol.* 84, 76–101. doi:10.1016/j.marpetgeo.2017.03.022

Li, H., Wang, Y., Zhu, W., Xu, Q., He, Y., Tang, W., et al. (2013). Seismic characteristics and processes of the Plio-Quaternary unidirectionally migrating channels and contourites in the northern slope of the South China Sea. *Mar. Petroleum Geol.* 43, 370–380. doi:10.1016/j.marpetgeo.2012.12.010

Liu, B., Pang, X., Yan, C., Liu, J., Lian, S., He, M., et al. (2011). Evolution of the Oligocene-Miocene shelf slope-break zone in the Baiyun deep-water area of the Pearl River Mouth Basin and its significance in oil-gas exploration. *Acta Pet. Sin.* 32 (2), 234–242. doi:10.7623/syxb201102007

Long, G., Shi, H., and Du, J. (2006). An analysis of creation conditions for Miocene stratigraphic and lithologic traps in Huizhou area, Pearl River Mouth basin. *China Offshore Oil Gas* 18 (4), 229–235.

Mitchum, R. M., Vail, P. R., and Sangree, J. B. (1977). "Seismic stratigraphy and global changes of sea-level, part 6: stratigraphic interpretation of seismic reflection patterns in depositional sequences," in *Seismic stratigraphy d applications to hydrocarbon exploration*. Editor C. E. Payton (Tulsa, Oklahoma: American Association of Petroleum Geologists Memoir), 117–133.

Mount, J. F. (1984). Mixing of siliciclastic and carbonate sediments in shallow shelf environments. *Geology* 12, 432–435. doi:10.1130/0091-7613(1984)12<432:MOSACS>2.0.CO;2

Neal, J., and Abreu, V. (2009). Sequence stratigraphy hierarchy and the accommodation succession method. *Geology* 37, 779–782. doi:10.1130/G25722A.1

Olariu, C., and Bhattacharya, J. P. (2006). Terminal distributary channels and delta front architecture of river-dominated delta systems. *J. Sediment. Res.* 76, 212–233. doi:10.2110/jsr.2006.026

Pang, X., Chen, C., and Peng, D. (2007a). *The Pearl River deep-water fan system and petroleum in south China sea*. Beijing: Science Press.

Pang, X., Chen, C., Shao, L., Wang, C., Zhu, M., He, M., et al. (2007b). Baiyun movement, a great tectonic event on the Oligocene-Miocene Boundary in the northern South China Sea and its implications. *Geol. Rev.* 53 (2), 145–151. doi:10.1016/S1872-5791(07)60044-X

Pang, X., Chen, C., Shi, H., Shu, Y., Shao, L., He, M., et al. (2005). Response between relative sea-level change and the Pearl River deep-water fan system in the South China Sea. *Earth Sci. Front.* 12 (3), 167–177. doi:10.3321/j.issn:1005-2321.2005.03.018

Posamentier, H. W. (2002). Ancient shelf ridges e a potentially significant component of the transgressive systems tract: case study from offshore northwest Java. *AAPG Bull.* 86, 75–106. doi:10.1306/61EEDA44-173E-11D7-8645000102C1865D

Posamentier, H. W., and Allen, G. P. (1999). *Siliciclastic sequence stratigraphy: concepts and applications*. Tulsa, Oklahoma: SEPM.

Qin, G. (1996). Application of micropaleontology to the sequence straitgprahy studies of late cenozoic in the Zhujiang River Mouth basin. *Mar. Geol. Quat. Geol.* 16 (4), 1–18. doi:10.16562/j.cnki.0256-1492.1996.04.001

Qin, G. (2002). Late cenozoic sequence stratigraphy and sea-level changes in Pearl River Mouth basin, south China sea. *China Offshore Oil Gas Geol.* 16 (1), 1–18.

Shabani, F., Amini, A., Tavakoli, V., Chehrazi, A., and Gong, C. (2023). 3D basin and petroleum system modelling of the early cretaceous play in the NW Persian Gulf. *Geoenergy Sci. Eng.* 226, 211768. doi:10.1016/j.geoen.2023.211768

Shabani, F., Amini, A., Tavakoli, V., Honarmand, J., and Gong, C. (2022). 3D forward stratigraphic modeling of the Albian succession in a part of the northeastern margin of the Arabian Plate and its implications for exploration of subtle traps. *Mar. Petroleum Geol.* 145, 105880. doi:10.1016/j.marpetgeo.2022.105880

Shao, L., Lei, Y., Pang, X., and Shi, H. (2005). Tectonic evolution and its controlling for sedimentary environment in Pearl River Mouth basin. *J. Tongji Univ. Nat. Sci.* 33 (9), 1177–1181.

Shao, L., Pang, X., Qiao, P., Chen, C., Li, Q., and Miao, W. (2008). Sedimentary filling of the Pearl River Mouth basin and its response to the evolution of the Pearl River. *Acta Sedmentologica Sin.* 26 (2), 179–184.

Shi, H., Dai, Y., Liu, L., Jiang, H., Li, H., and Bai, J. (2015). Geological characteristics and distribution model of oil and gas reservoirs in Zhu - depression, Pearl River Mouth basin. *Acta Pet. Sin.* 36 (2), 120–132. doi:10.7623/syxb2015S2011

Shi, H., Qin, C., Gao, P., Zhang, Z., Zhu, J., and Zhao, R. (2008). Late gas accumulation characteristics in Panyu low-uplift and the north slope of Baiyun sag, Pearl River Mouth Basin. *China Offshore Oil Gas* 20 (2), 73–76.

Shi, H., Zhu, J., Jiang, Z., Shu, Y., Xie, T., and Wu, J. (2009). Hydrocarbon resources reassessment in Zhu I depression, Pearl River Mouth basin. *China Offshore Oil Gas* 21 (1), 9–14.

Sun, Z., Zhong, Z., Keep, M., Zhou, D., Cai, D., Li, X., et al. (2009). 3D analogue modeling of the South China Sea: a discussion on breakup pattern. *J. Asian Earth Sci.* 34, 544–556. doi:10.1016/j.jseaes.2008.09.002

Suter, J. R. (2006). "Facies models revisited: clastic shelves," in *Facies models revisited*. Editors H. W. Posamentier and R. G. Walker (Tulsa, Oklahoma: SEPM), 339–397.

Tavakoli, V. (2017). Application of gamma deviation log (GDL) in sequence stratigraphy of carbonate strata, an example from offshore Persian Gulf, Iran. *J. Petroleum Sci. Eng.* 156, 868–876. doi:10.1016/j.petrol.2017.06.069

Tavakoli, V., Naderi-Khujin, M., and Seyedmehdi, Z. (2018). The end-Permian regression in the western Tethys: sedimentological and geochemical evidence from offshore the Persian Gulf, Iran. *Geo-Marine Lett.* 38 (2), 179–192. doi:10.1007/s00367-017-0520-8

Vail, P. R., Mitchum, R. M., Jr., and Thompson, S., III (1977). "Seismic stratigraphy and global changes of sea level, part 3: relative changes of sea level from coastal onlap," in *Seismic stratigraphyeapplications to hydrocarbon exploration*. Editor C. E. Payton (Tulsa, Oklahoma: American Association of Petroleum Geologists), 63–81.

Van Wagoner, J. C., Posamentier, H. W., Mitchum, R. M., Jr., Vail, P. R., Sarg, J. F., Loutit, T. S., et al. (1988). "An overview of sequence stratigraphy and key definitions," in *Sea level ChangeseAn integrated approach*. Editors C. K. Wilgus, B. S. Hastings, C. G. St, C. Kendall, H. W. Posamentier, C. A. Ross, et al. (Tulsa, Oklahoma: SEPM), 39–45.

Walker, R. G., and Bergman, K. M. (1993). Shannon sandstone in Wyoming: a shelf ridge complex reinterpreted as lowstand shoreface deposits. *J. Sediment. Res.* 63, 839–851. doi:10.1306/D4267C21-2B26-11D7-8648000102C1865D

Wei, Z., Li, X., Hao, Y., Zeng, Y., Zhou, X., and Xiang, Q. (2022). Mixed sedimentary characteristics and exploration potential of Dongsha uplift in Pearl River Mouth basin. *Complex Hydrocarb. Reserv.* 15, 38–43. doi:10.16181/j.cnki.fzyqc.2022.03.007

Zecchin, M., and Catuneanu, O. (2017). High-resolution sequence stratigraphy of clastic shelves VI: mixed siliciclastic-carbonate systems. *Mar. Petroleum Geol.* 88, 712–723. doi:10.1016/j.marpetgeo.2017.09.012

Zhang, G., Mi, L., Tao, W., and Lü, J. (2007). Deepwater area – the new prospecting targets of northern continental margin of South China Sea. *Acta Pet. Sin.* 28 (2), 15–21. doi:10.7623/syxb200206003

Zhang, X., Li, X., Du, J., Ding, L., Li, X., Wu, Y., et al. (2021). Mixed siliciclastic-carbonate sedimentation on the Miocene Pearl River continental shelf, northeastern South China Sea: implications for exploring lithologic traps. *Interpretation* 9 (2), SC31–SC43. doi:10.1190/INT-2020-0162.1

Zhong, J. (1994). Characteristics of geologic structure and basin evolution in Pearl Riverriver Mouth Basin. *Trans. Oceanol. Limnol.* 1, 1–8. doi:10.13984/j.cnki.cn37-1141.1994.01.001

Zhuo, H., Wang, Y., Shi, H., Zhu, M., He, M., Chen, W., et al. (2014). Seismic geomorphology, architecture and genesis of Miocene shelf sand ridges in the Pearl River Mouth Basin, northern South China sea. *Mar. Petroleum Geol.* 54, 106–122. doi:10.1016/j.marpetgeo.2014.03.002

Zhuo, H., Wang, Y., Sun, Z., Wang, Y., Xu, Q., Hou, P., et al. (2019). Along-strike variability in shelf-margin morphology and accretion pattern: an example from the northern margin of the South China Sea. *Basin Res.* 31 (3), 431–460. doi:10.1111/bre.12329

Zonneveld, J. P., Gingras, M. K., Beatty, T. W., Bottjer, D. J., Chaplin, J. R., Greene, S. E., et al. (2012). "Mixed siliciclastic/carbonate systems," in *Trace fossils as indicators of sedimentary environments*. Editors D. Knaust and R. G. Bromley (Amsterdam: Elsevier), 807–833.